

$h \rightarrow \gamma\gamma$ in $U(1)_R$ – lepton number model with a right-handed neutrino

Sabyasachi Chakraborty,^{a,1} Asesh Krishna Datta,^b Sourov Roy^a

^a*Department of Theoretical Physics, Indian Association for the Cultivation of Science, 2A & 2B Raja S.C.Mullick Road, Jadavpur, Kolkata 700 032, INDIA*

^b*Harish-Chandra Research Institute, Chhatnag Road, Jhansi, Allahabad 211019, INDIA*

E-mail: tpsc3@iacs.res.in, asesh@hri.res.in, tpsr@iacs.res.in

ABSTRACT: We perform a detailed study of the signal rate of the lightest Higgs boson in the diphoton channel ($\mu_{\gamma\gamma}$), recently analyzed by both the ATLAS and CMS collaborations at the Large Hadron Collider, in the framework of $U(1)_R$ – lepton number model with a right handed neutrino superfield. The corresponding neutrino Yukawa coupling, ‘ f ’, plays a very important role in the phenomenology of this model. A large value of $f \sim \mathcal{O}(1)$ provides an additional tree level contribution to the lightest Higgs boson mass along with a very light (mass \sim a few hundred MeV) bino like neutralino and a small tree level mass of one of the active neutrinos that is compatible with various experimental results. In the presence of this light neutralino, the invisible decay width of the Higgs boson can become important. We studied this scenario in conjunction with the recent LHC results. The signal rate $\mu_{\gamma\gamma}$ obtained in this scenario is compatible with the recent results from both the ATLAS and the CMS collaborations at 1σ level. A small value of ‘ f ’, on the other hand, is compatible with a sterile neutrino acting as a 7 keV dark matter that can explain the observation of a mono-energetic X-ray photon line by the XMM-Newton X-ray observatory. We also study the impact of $\mu_{\gamma\gamma}$ in this case.

KEYWORDS: Supersymmetry Phenomenology

¹Corresponding author.

Contents

1	Introduction	1
2	$U(1)_R$-lepton number model with a right handed neutrino	4
3	The scalar sector	6
3.1	CP-even neutral scalar sector	7
3.2	Tree level mass bound on m_h	8
4	The fermionic sector	10
4.1	The neutralino sector: R-conserving case	11
4.2	The neutralino sector: R-breaking case	11
4.3	The chargino sector	14
5	Contributions to $\mu_{\gamma\gamma}$	15
5.1	The decay $h \rightarrow gg$	16
5.2	The decay $h \rightarrow \gamma\gamma$	17
5.3	Higgs boson decaying to charginos and neutralinos	20
5.4	The total decay width of the Higgs boson	22
6	Impact of the LHC results	22
6.1	The case of large neutrino Yukawa coupling, $f \sim \mathcal{O}(1)$	22
6.1.1	Invisible branching ratio of the Higgs boson	23
6.1.2	The signal strength $\mu_{\gamma\gamma}$	24
6.1.3	Relative signal strengths in different final states	25
6.2	The case of small Yukawa coupling, $f \sim \mathcal{O}(10^{-4})$	27
7	Concluding remarks	30
A	The Higgs-chargino-chargino coupling	31
B	The Higgs-neutralino-neutralino coupling	35

1 Introduction

Recently two CERN based Large Hadron Collider (LHC) experiments, ATLAS and CMS, have confirmed the existence of a neutral boson, widely accepted to be the Higgs boson, an elementary scalar boson of nature [1, 2], with mass around 125 GeV. Almost all the decay channels have been probed with reasonable precision. Out of these, results in the $h \rightarrow \gamma\gamma$ channel have attracted a lot of attention in recent times. The reason is two-fold: first,

this is the discovery mode of the Higgs boson and second, being a loop induced process it may potentially carry indirect hints of new physics. The results reported so far show some deviations with respect to the Standard Model (SM) prediction. For example, the ATLAS collaboration reported $\mu_{\gamma\gamma} = 1.17 \pm 0.27$ [3], where $\mu_{\gamma\gamma} = \frac{\sigma(pp \rightarrow h \rightarrow \gamma\gamma)}{\sigma(pp \rightarrow h \rightarrow \gamma\gamma)^{SM}}$. On the other hand, CMS collaboration reported a best-fit signal strength in their main analysis [4] where, $\mu_{\gamma\gamma} = 1.14_{-0.23}^{+0.26}$. Moreover, a cut-based analysis by CMS produced a slightly different value, which is quoted as $\mu_{\gamma\gamma} = 1.29_{-0.26}^{+0.29}$. This enhancement or suppression in the $h \rightarrow \gamma\gamma$ channel with respect to the SM provide a natural testing ground for physics Beyond the SM (BSM). Detailed studies have already been carried out for this particular channel. For example, $h \rightarrow \gamma\gamma$ is studied in a wide variety of supersymmetric (SUSY) models namely, the minimal supersymmetric standard model (MSSM) [5–25], its next-to-minimal version (NMSSM) [26–34], the constrained MSSM (CMSSM) [35–40] and also in (B-L)SSM [41–44], left-right supersymmetric models [45], and in $U(1)'$ extension of MSSM [46]. In [47], a triplet-singlet extension of MSSM has been studied and $\mu_{\gamma\gamma}$ is computed.

Motivated by these results we would like to investigate the Higgs to diphoton mode in the context of a supersymmetric scenario known as $U(1)_R$ – lepton number model, which is augmented by a single right-handed neutrino superfield. It is rather well known that supersymmetry is one of the very popular frameworks that provides a suitable dark matter candidate and can also explain the origin of neutrino masses and mixing. However, the non-observation of superpartners so far has already put stringent lower bounds on their masses in different SUSY models, subject to certain assumptions. In the light of these constraints, R -symmetric models which generically contain Dirac gauginos in their spectra (as opposed to Majorana gauginos in usual SUSY scenarios) are very well motivated. In particular, the presence of Dirac gluino in this class of models reduces the squark production cross section compared to MSSM thus relaxing the bound on squark masses. Detailed studies on R -symmetric models and Dirac gauginos can be found in the literature [48–98]. Flavor and CP violating constraints are also suppressed in these class of models [58]. To construct Dirac gaugino masses, the gauge sector of the supersymmetric Standard Model has to be extended to incorporate chiral superfields in the adjoint representations of the SM gauge group. A singlet \hat{S} , an $SU(2)$ triplet \hat{T} and an $SU(3)$ octet \hat{O} , help obtain the Dirac gaugino masses.

In this paper we consider the minimal extension of a specific $U(1)_R$ symmetric model [84, 85] by introducing a right handed neutrino superfield [88]. In such a scenario the R-charges are identified with lepton numbers such that the lepton number of SM fermions and their superpartners are negative of the corresponding R-charges. Such an identification leaves the lepton number assignments of the SM fermions unchanged from the usual ones while the same for the superpartners become non-standard. This has an interesting consequence for the sneutrinos which now do not carry any lepton number. Hence, although in this model sneutrinos get non-zero vacuum expectation value (vev) in general, the latter do not get constrained from neutrino Majorana masses which require lepton number violation by two units. A sneutrino thus can play the role of a down type Higgs boson, a phenomenon which has crucial implications [74, 79, 84, 85, 88] for our purpose that we would discuss later in this work. The right handed neutrino, on the other hand, not only provides a small

tree level Dirac neutrino mass but also gives rise to an additional tree level contribution to the Higgs boson mass proportional to the neutrino Yukawa coupling [88]. When the R-symmetry is broken, a small ($\lesssim 0.05$ eV) Majorana mass for one of the active neutrinos is generated at the tree level while the right handed sterile neutrino can have keV Majorana mass and can be accommodated as a warm dark matter candidate ¹.

A large Yukawa coupling $f \sim \mathcal{O}(1)$ facilitates having the mass of the lightest Higgs boson around 125 GeV without resorting to radiative contributions. Large values of f also result in a very light neutralino with mass around a few hundred MeV. Cosmological implications of having such a light neutralino is briefly discussed in ref. [88] for this model. Some general studies regarding light neutralinos can be found in [100–109]. On the other hand, in the regime of small Yukawa coupling $f \sim 10^{-4}$, the Higgs boson mass is devoid of any large tree level contribution. Therefore, to obtain the mass of the lightest Higgs boson in the right ballpark, radiative corrections have to be incorporated, which are required to be large enough. This can be achieved either by having large singlet and triplet couplings [62], $\lambda_S, \lambda_T \sim \mathcal{O}(1)$, or by having a large top squark mass.

In this work, we study the implications of such a scenario with particular reference to the diphoton final states arising from the decay of the lightest Higgs boson. We study this scenario in conjunction with the recent results of $\mu_{\gamma\gamma}$ obtained from the latest results of LHC collaborations. This particular case under consideration has some important implications since we can now afford rather light top squarks which potentially affect the resonant production rate of the lightest Higgs boson and its decay pattern. Furthermore, presence of a very light neutralino opens up new decay modes of the Higgs bosons which in turn is subject to the constraints from Higgs invisible branching fractions. Also, in general, presence of new particle states and their involved couplings would affect the proceedings.

The plan of the work is as follows. In Section 2 we briefly discuss the main features of the model. The principal motivation and the artifacts of the $U(1)_R$ - lepton number model are also discussed with reference to its scalar and the electroweak gaugino sector. In section 3, we discuss the scalar sector of the model in detail. In Section 4 we address the neutralino and the chargino sectors. The masses and the couplings in these sectors play important roles in the computation of $\mu_{\gamma\gamma}$. A thorough analysis of $\mu_{\gamma\gamma}$ requires the knowledge of both production and decays of the Higgs boson. In Section 5 issues pertaining to the production of Higgs boson in the present scenario is discussed in some detail. Analytical expressions of Higgs boson decaying to two photons in our model are also given in the same section. Section 6 is dedicated to the computation of the invisible decay width of the Higgs boson. Here we also discuss the impact of the findings from the LHC pertaining to the Higgs sector on the scenario under discussion for two distinct cases: a) when the neutrino Yukawa coupling is large, i.e., $\mathcal{O}(1)$ and b) when it is $\mathcal{O}(10^{-4})$. We also provide $\mu_{\gamma\gamma}$ and show its variation with relevant parameters, along with the points representing the 7 keV sterile neutrino warm dark matter in this model. We conclude in Section 7 with some future outlooks. The Higgs boson couplings to neutralino and charginos in this model are relegated to the appendix.

¹For a review on other models of keV sterile neutrino dark matter, see ref. [99].

2 $U(1)_R$ -lepton number model with a right handed neutrino

We consider a minimal extension of an R -symmetric model, first discussed in [84, 85], by extending the field content with a single right handed neutrino superfield [88]. Along with the MSSM superfields, $\hat{H}_u, \hat{H}_d, \hat{U}_i^c, \hat{D}_i^c, \hat{L}_i, \hat{E}_i^c$, two inert doublet superfields \hat{R}_u and \hat{R}_d with opposite hypercharge are considered in addition to the right handed neutrino superfield \hat{N}^c . These two doublets \hat{R}_u and \hat{R}_d carry non zero R -charges (The R -charge assignments are provided in table 1 and therefore, in order to avoid spontaneous R -breaking and the emergence of R -axions, the scalar components of \hat{R}_u and \hat{R}_d do not receive any nonzero vev and because of this they are coined as inert doublets.

	\hat{Q}_i	\hat{U}_i^c	\hat{D}_i^c	\hat{L}_i	\hat{E}_i^c	\hat{H}_u	\hat{H}_d	\hat{R}_u	\hat{R}_d	\hat{S}	\hat{T}	\hat{O}	\hat{N}^c
$U(1)_R$	1	1	1	0	2	0	0	2	2	0	0	0	2

Table 1. $U(1)_R$ charge assignments of the chiral superfields.

R -symmetry prohibits the gauginos to have Majorana mass term and trilinear scalar interactions (A -terms) are also absent in a $U(1)_R$ invariant scenario. However, the gauginos can acquire Dirac masses. In order to have Dirac gaugino masses one needs to include chiral superfields in the adjoint representations of the standard model gauge group. Namely a singlet \hat{S} , an $SU(2)_L$ triplet \hat{T} and an octet \hat{O} under $SU(3)_c$. These chiral superfields are essential to provide Dirac masses to the bino, wino and gluino respectively. We would like to reiterate that the lepton numbers have been identified with the (negative) of R -charges such that the lepton number of the SM fermions are the usual ones whereas the superpartners of the SM fermions carry *non-standard* lepton numbers. With such lepton number assignments this R -symmetric model is also lepton number conserving [84, 85, 88].

The generic superpotential carrying an R -charge of two units can be written as

$$\begin{aligned}
W = & y_{ij}^u \hat{H}_u \hat{Q}_i \hat{U}_j^c + \mu_u \hat{H}_u \hat{R}_d + f_i \hat{L}_i \hat{H}_u \hat{N}^c + \lambda_S \hat{S} \hat{H}_u \hat{R}_d + 2\lambda_T \hat{H}_u \hat{T} \hat{R}_d - M_R \hat{N}^c \hat{S} + \mu_d \hat{R}_u \hat{H}_d \\
& + \lambda'_S \hat{S} \hat{R}_u \hat{H}_d + \lambda_{ijk} \hat{L}_i \hat{L}_j \hat{E}_k^c + \lambda'_{ijk} \hat{L}_i \hat{Q}_j \hat{D}_k^c + 2\lambda'_T \hat{R}_u \hat{T} \hat{H}_d + y_{ij}^d \hat{H}_d \hat{Q}_i \hat{D}_j^c + y_{ij}^e \hat{H}_d \hat{L}_i \hat{E}_j^c \\
& + \lambda_N \hat{N}^c \hat{H}_u \hat{H}_d.
\end{aligned} \tag{2.1}$$

For simplicity, in this work we have omitted the terms $\kappa \hat{N}^c \hat{S} \hat{S}$ and $\eta \hat{N}^c$ from the superpotential. As long as $\eta \sim M_{SUSY}^2$ and $\kappa \sim 1$ we do not expect any significant change in the analysis and the results presented in this paper.

In order to have a realistic model one should also include supersymmetric breaking terms, which are the scalar and the gaugino mass terms. The Lagrangian containing the Dirac gaugino masses can be written as [71, 73]

$$\mathcal{L}_{\text{gaugino}}^{\text{Dirac}} = \int d^2\theta \frac{W'_\alpha}{\Lambda} [\sqrt{2}\kappa_1 W_{1\alpha} \hat{S} + 2\sqrt{2}\kappa_2 \text{tr}(W_{2\alpha} \hat{T}) + 2\sqrt{2}\kappa_3 \text{tr}(W_{3\alpha} \hat{O})] + h.c., \tag{2.2}$$

where $W'_\alpha = \lambda_\alpha + \theta_\alpha D'$ is a spurion superfield parametrizing D -type supersymmetry breaking. This results in Dirac gaugino masses as D' acquires vev and are given by

$$M_i^D = \kappa_i \frac{\langle D' \rangle}{\Lambda}, \tag{2.3}$$

where Λ denotes the scale of SUSY breaking mediation and κ_i are order one coefficients.

It is worthwhile to note that these Dirac gaugino mass terms have been dubbed as ‘supersoft’ terms. This is because we know that the Majorana gaugino mass terms generate logarithmic divergence to the scalar masses whereas in ref. [54], it was shown that the purely scalar loop, obtained from the adjoint superfields cancels this logarithmic divergence in the case of Dirac gauginos. Hence it is not unnatural to consider the Dirac gaugino masses to be rather large.

The R-conserving but soft supersymmetry breaking terms in the scalar sector are generated from a spurion superfield \hat{X} , where $\hat{X} = x + \theta^2 F_X$ such that $R[\hat{X}] = 2$ and $\langle x \rangle = 0$, $\langle F_X \rangle \neq 0$. The non-zero vev of F_X generates the scalar soft terms and the corresponding potential is given by

$$\begin{aligned}
V_{soft} = & m_{H_u}^2 H_u^\dagger H_u + m_{R_u}^2 R_u^\dagger R_u + m_{H_d}^2 H_d^\dagger H_d + m_{R_d}^2 R_d^\dagger R_d + m_{\tilde{L}_i}^2 \tilde{L}_i^\dagger \tilde{L}_i + m_{\tilde{R}_i}^2 \tilde{R}_i^\dagger \tilde{R}_i \\
& + M_N^2 \tilde{N}^{c\dagger} \tilde{N}^c + m_S^2 S^\dagger S + 2m_T^2 \text{tr}(T^\dagger T) + 2m_O^2 \text{tr}(O^\dagger O) + (B\mu H_u H_d + \text{h.c.}) \\
& - (b\mu_L^i H_u \tilde{L}_i + \text{h.c.}) + (t_S S + \text{h.c.}) + \frac{1}{2} b_S (S^2 + \text{h.c.}) + b_T (\text{tr}(TT) + \text{h.c.}) \\
& + B_O (\text{tr}(OO) + \text{h.c.}).
\end{aligned} \tag{2.4}$$

The presence of the bilinear terms $b\mu_L^i H_u \tilde{L}_i$ implies that all the three left handed sneutrinos can acquire non-zero vev 's. However, it is always possible to make a basis rotation in which only one of the left handed sneutrinos get a non-zero vev and one must keep in mind that the physics is independent of this basis choice.

Such a rotation can be defined as

$$\hat{L}_i = \frac{v_i}{v_a} \hat{L}_a + \sum_b e_{ib} \hat{L}_b. \tag{2.5}$$

Note that the index (i) runs over three generations whereas $a = 1(e)$ and $b = 2, 3(\mu, \tau)$. This basis rotation implies that the scalar component of the superfield \hat{L}_a acquires a non zero vev (i.e. $\langle \tilde{\nu} \rangle \equiv v_a \neq 0$) whereas the other two sneutrinos do not get any vev . One can further go to a basis where the charged lepton Yukawa couplings are diagonal. It is, however, important to note that the charged lepton of flavor a (i.e. the electron) cannot get mass from this Yukawa couplings because of $SU(2)_L$ invariance but can be generated from R-symmetric supersymmetry breaking operators [84]. Moreover, we also choose the neutrino Yukawa coupling in such a way that only \hat{L}_a couples to² \hat{N}^c . In such a scenario the left-handed sneutrino can play the role of a down type Higgs boson since its vev preserves lepton number and is not constrained by neutrino Majorana mass. Hence one has the freedom to keep a very large μ_d such that the superfields \hat{H}_d and \hat{R}_u get decoupled from the theory. This is what we shall consider in the rest of our discussion.

With a single sneutrino acquiring a vev and in the mass eigenstate basis of the charged lepton and down type quark fields the superpotential now has the following form (integrating out \hat{H}_d and \hat{R}_u)

$$\begin{aligned}
W = & y_{ij}^u \hat{H}_u \hat{Q}_i \hat{U}_j^c + \mu_u \hat{H}_u \hat{R}_d + f \hat{L}_a \hat{H}_u \hat{N}^c + \lambda_S \hat{S} \hat{H}_u \hat{R}_d + 2\lambda_T \hat{H}_u \hat{T} \hat{R}_d \\
& - M_R \hat{N}^c \hat{S} + W',
\end{aligned} \tag{2.6}$$

²For a detailed discussion we refer the reader to ref. [88].

where

$$\begin{aligned}
W' = & \sum_{b=2,3} f_b^l \hat{L}_a \hat{L}'_b \hat{E}'_b{}^c + \sum_{k=1,2,3} f_k^d \hat{L}_a \hat{Q}'_k \hat{D}'_k{}^c \\
& + \sum_{k=1,2,3} \frac{1}{2} \tilde{\lambda}_{23k} \hat{L}'_2 \hat{L}'_3 \hat{E}'_k{}^c + \sum_{j,k=1,2,3;b=2,3} \tilde{\lambda}'_{bjk} \hat{L}'_b \hat{Q}'_j \hat{D}'_k{}^c,
\end{aligned} \tag{2.7}$$

and includes all the trilinear R-parity violating terms in this model. In the subsequent discussion we shall confine ourselves to this choice of basis but get rid of the primes from the fields and make the replacement $\tilde{\lambda}, \tilde{\lambda}' \rightarrow \lambda, \lambda'$.

In this rotated basis the soft supersymmetry breaking terms look like

$$\begin{aligned}
V_{soft} = & m_{H_u}^2 H_u^\dagger H_u + m_{R_d}^2 R_d^\dagger R_d + m_{\tilde{L}_a}^2 \tilde{L}_a^\dagger \tilde{L}_a + \sum_{b=2,3} m_{\tilde{L}_b}^2 \tilde{L}_b^\dagger \tilde{L}_b + M_N^2 \tilde{N}^{c\dagger} \tilde{N}^c + m_{\tilde{R}_i}^2 \tilde{l}_{Ri}^\dagger \tilde{l}_{Ri} \\
& + m_{\tilde{S}}^2 S^\dagger S + 2m_T^2 \text{tr}(T^\dagger T) + 2m_O^2 \text{tr}(O^\dagger O) - (b\mu_L H_u \tilde{L}_a + \text{h.c.}) + (t_S S + \text{h.c.}) \\
& + \frac{1}{2} b_S (S^2 + \text{h.c.}) + b_T (\text{tr}(TT) + \text{h.c.}) + B_O (\text{tr}(OO) + \text{h.c.}).
\end{aligned} \tag{2.8}$$

With this short description of the theoretical framework let us now explore the scalar and the fermionic sectors in some detail in order to prepare the ground for the study of the diphoton decay of the lightest Higgs boson.

3 The scalar sector

The scalar potential receives contributions from the F-term, the D-term, the soft SUSY breaking terms and the terms coming from one-loop radiative corrections. Thus, schematically,

$$V = V_F + V_D + V_{soft} + V_{\text{one-loop}}. \tag{3.1}$$

The F-term contribution is given by

$$V_F = \sum_i \left| \frac{\partial W}{\partial \phi_i} \right|^2, \tag{3.2}$$

where the superpotential W is given by eq. (2.6). The D-term contribution can be written as

$$V_D = \frac{1}{2} \sum_a D^a D^a + \frac{1}{2} D_Y D_Y, \tag{3.3}$$

where

$$D^a = g(H_u^\dagger \tau^a H_u + \tilde{L}_i^\dagger \tau^a \tilde{L}_i + T^\dagger \lambda^a T) + \sqrt{2}(M_2^D T^a + M_2^D T^{a\dagger}). \tag{3.4}$$

The τ^a 's and λ^a 's are the $SU(2)$ generators in the fundamental and adjoint representation respectively. The weak hypercharge contribution D_Y is given by

$$D_Y = \frac{g'}{2}(H_u^+ H_u - \tilde{L}_i^+ \tilde{L}_i) + \sqrt{2} M_1^D (S + S^\dagger), \tag{3.5}$$

where g and g' are $SU(2)_L$ and $U(1)_Y$ gauge couplings respectively. The expanded forms of V_F and V_D in terms of various scalar fields can be found in [88]. The soft SUSY breaking term V_{soft} is given in Eq. (2.8) whereas the dominant radiative corrections to the quartic potential are of the form $\frac{1}{2}\delta\lambda_u(|H_u|^2)^2$, $\frac{1}{2}\delta\lambda_\nu(|\tilde{\nu}_a|^2)^2$ and $\frac{1}{2}\delta\lambda_3|H_u^0|^2|\tilde{\nu}_a|^2$. The coefficients $\delta\lambda_u$, $\delta\lambda_\nu$ and $\delta\lambda_3$ are given by

$$\begin{aligned} \delta\lambda_u &= \frac{3y_t^4}{16\pi^2} \ln\left(\frac{m_{\tilde{t}_1} m_{\tilde{t}_2}}{m_t^2}\right) + \frac{5\lambda_T^4}{16\pi^2} \ln\left(\frac{m_T^2}{v^2}\right) + \frac{\lambda_S^4}{16\pi^2} \ln\left(\frac{m_S^2}{v^2}\right) \\ &\quad - \frac{1}{16\pi^2} \frac{\lambda_S^2 \lambda_T^2}{m_T^2 - m_S^2} \left(m_T^2 \left\{ \ln\left(\frac{m_T^2}{v^2}\right) - 1 \right\} - m_S^2 \left\{ \ln\left(\frac{m_S^2}{v^2}\right) - 1 \right\} \right), \end{aligned} \quad (3.6)$$

$$\begin{aligned} \delta\lambda_\nu &= \frac{3y_b^4}{16\pi^2} \ln\left(\frac{m_{\tilde{b}_1} m_{\tilde{b}_2}}{m_b^2}\right) + \frac{5\lambda_T^4}{16\pi^2} \ln\left(\frac{m_T^2}{v^2}\right) + \frac{\lambda_S^4}{16\pi^2} \ln\left(\frac{m_S^2}{v^2}\right) \\ &\quad - \frac{1}{16\pi^2} \frac{\lambda_S^2 \lambda_T^2}{m_T^2 - m_S^2} \left(m_T^2 \left\{ \ln\left(\frac{m_T^2}{v^2}\right) - 1 \right\} - m_S^2 \left\{ \ln\left(\frac{m_S^2}{v^2}\right) - 1 \right\} \right), \end{aligned} \quad (3.7)$$

$$\begin{aligned} \delta\lambda_3 &= \frac{5\lambda_T^4}{32\pi^2} \ln\left(\frac{m_T^2}{v^2}\right) + \frac{1}{32\pi^2} \lambda_S^4 \ln\left(\frac{m_S^2}{v^2}\right) + \frac{1}{32\pi^2} \frac{\lambda_S^2 \lambda_T^2}{m_T^2 - m_S^2} \left(m_T^2 \left\{ \ln\left(\frac{m_T^2}{v^2}\right) - 1 \right\} \right. \\ &\quad \left. - m_S^2 \left\{ \ln\left(\frac{m_S^2}{v^2}\right) - 1 \right\} \right). \end{aligned} \quad (3.8)$$

We shall see later that for large values of the couplings λ_T and λ_S or large stop masses these one-loop radiative contributions to the Higgs quartic couplings could play important roles in obtaining a CP-even lightest Higgs boson with a mass around 125 GeV.

3.1 CP-even neutral scalar sector

Let us assume that the neutral scalar fields H_u^0 , $\tilde{\nu}_a$ ($a = 1(e)$), S and T acquire real vacuum expectation values v_u , v_a , v_S and v_T , respectively. The scalar fields R_d and \tilde{N}^c carrying R-charge 2 are decoupled from these four scalar fields. We can split the fields in terms of their real and imaginary parts: $H_u^0 = h_R + ih_I$, $\tilde{\nu}^a = \tilde{\nu}_R^a + i\tilde{\nu}_I^a$, $S = S_R + iS_I$ and $T = T_R + iT_I$. The resulting minimization equations can be found easily and with the help of these minimization equations, the neutral CP-even scalar squared-mass matrix in the basis $(h_R, \tilde{\nu}_R, S_R, T_R)$ can be written down in a straightforward way, where h_4 corresponds to the lightest CP even mass eigenstate [88]. In the R-symmetry preserving scenario the

elements of this symmetric 4×4 matrix are found to be

$$\begin{aligned}
(M_S^2)_{11} &= \frac{(g^2 + g'^2)}{2} v^2 \sin^2 \beta + (f M_{RvS} - b\mu_L^a)(\tan \beta)^{-1} + 2\delta\lambda_u v^2 \sin^2 \beta, \\
(M_S^2)_{12} &= f^2 v^2 \sin 2\beta + b\mu_L^a - \frac{(g^2 + g'^2 - 2\delta\lambda_3)}{4} v^2 \sin 2\beta - f M_{RvS}, \\
(M_S^2)_{13} &= 2\lambda_S^2 v_S v \sin \beta + 2\mu_u \lambda_S v \sin \beta + 2\lambda_S \lambda_T v v_T \sin \beta + \sqrt{2} g' M_1^D v \sin \beta - f M_{Rv} \cos \beta, \\
(M_S^2)_{14} &= 2\lambda_T^2 v_T v \sin \beta + 2\mu_u \lambda_T v \sin \beta + 2\lambda_S \lambda_T v_S v \sin \beta - \sqrt{2} g M_2^D v \sin \beta, \\
(M_S^2)_{22} &= \frac{(g^2 + g'^2)}{2} v^2 \cos^2 \beta + (f M_{RvS} - b\mu_L^a) \tan \beta + 2\delta\lambda_\nu v^2 \cos^2 \beta, \\
(M_S^2)_{23} &= -\sqrt{2} g' M_1^D v \cos \beta - f M_{Rv} \sin \beta, \\
(M_S^2)_{24} &= \sqrt{2} g M_2^D v \cos \beta, \\
(M_S^2)_{33} &= -\mu_u \lambda_S \frac{v^2 \sin^2 \beta}{v_S} - \frac{\lambda_S \lambda_T v_T v^2 \sin^2 \beta}{v_S} - \frac{t_S}{v_S} + \frac{g' M_1^D v^2 \cos 2\beta}{\sqrt{2} v_S} + \frac{f M_{Rv} v^2 \sin 2\beta}{2v_S}, \\
(M_S^2)_{34} &= \lambda_S \lambda_T v^2 \sin^2 \beta, \\
(M_S^2)_{44} &= -\mu_u \lambda_T \frac{v^2}{v_T} \sin^2 \beta - \lambda_S \lambda_T v_S \frac{v^2}{v_T} \sin^2 \beta - \frac{g M_2^D v^2}{\sqrt{2} v_T} \cos 2\beta, \tag{3.9}
\end{aligned}$$

where $\tan \beta = v_u/v_a$ and $v^2 = v_u^2 + v_a^2$. The W^\pm - and the Z -boson masses can be written as

$$\begin{aligned}
m_W^2 &= \frac{1}{2} g^2 (v^2 + 4v_T^2), \\
m_Z^2 &= \frac{1}{2} g^2 v^2 / \cos^2 \theta_W. \tag{3.10}
\end{aligned}$$

Note that the electroweak precision measurements of the ρ -parameter requires that the triplet vev v_T must be small ($\lesssim 3$ GeV) [110]. In addition, our requirement of a doublet-like lightest CP-even Higgs boson, in turn, demands a small vev v_S of the singlet S as well. This is because a small value of v_S reduces the mixing between the doublets and the singlet scalar S . In such a simplified but viable scenario in which the singlet and the $SU(2)_L$ triplet scalars get decoupled from the theory, we are left with a 2×2 scalar mass matrix. In this case the angle α represents the mixing angle between h_R and $\tilde{\nu}_R$ and can be expressed in terms of other parameters as follows

$$\tan 2\alpha = -2 \frac{f^2 v^2 \sin 2\beta + b\mu_L^a - \frac{(g^2 + g'^2 - 2\delta\lambda_3)}{4} v^2 \sin 2\beta}{\frac{(g^2 + g'^2) v^2 \cos 2\beta}{2} + 2b\mu_L^a \cot 2\beta - 2v^2 \{ \delta\lambda_u \sin^2 \beta - \delta\lambda_\nu \cos^2 \beta \}}. \tag{3.11}$$

3.2 Tree level mass bound on m_h

In addition, in such a situation (with $v_S, v_T \ll v$) it can be shown easily that the lightest CP-even Higgs boson mass is bounded from above at tree level [88],

$$(m_h^2)_{\text{tree}} \leq m_z^2 \cos^2 2\beta + f^2 v^2 \sin^2 2\beta. \tag{3.12}$$

The bound in Eq. (3.12) is saturated for $v_s \lesssim 10^{-3}$ GeV, i.e., when the singlet has a large soft supersymmetry breaking mass and is integrated out. The $f^2 v^2$ term grows at

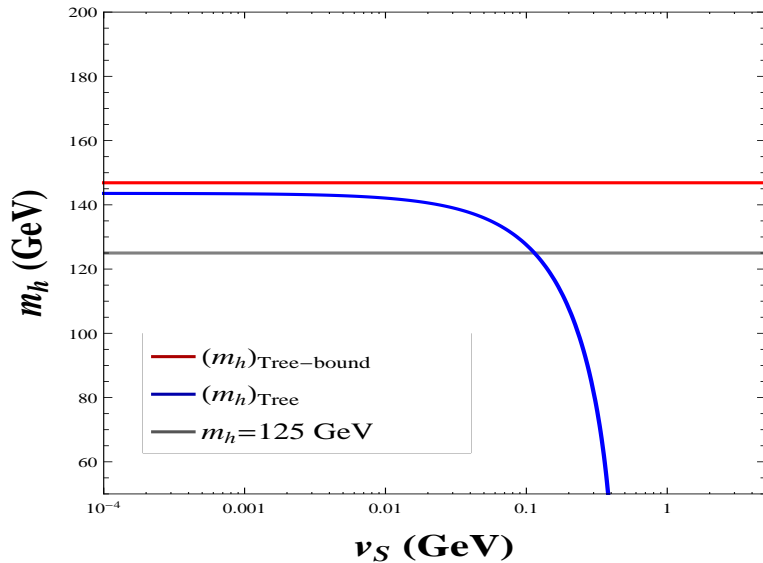


Figure 1. The tree level mass of the lightest Higgs boson as a function of the singlet (S) vacuum expectation value v_S with $f = 1.5$, $\tan\beta = 4$ and other parameter choices are as described in the text. The upper bound on the tree level mass of the Higgs boson from eq. 3.12 is also shown.

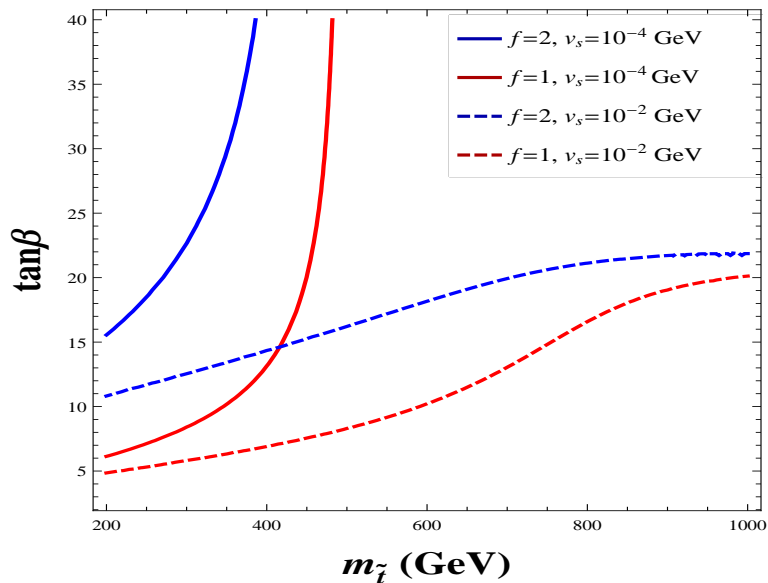


Figure 2. Mass-contours for the lightest Higgs boson with $m_h = 125$ GeV in the $m_{\tilde{t}} - \tan\beta$ plane for large values of f and $\lambda_T = 0.5$.

small $\tan\beta$ and thus the largest Higgs boson mass is obtained with low $\tan\beta$ and large values of f . We shall show in the next section that $f \sim 1$ can be accommodated in this scenario without spoiling the smallness of the neutrino mass at tree level. Therefore, for $f \sim \mathcal{O}(1)$, the tree level Higgs boson mass can be as large as ~ 125 GeV where the peak in

the diphoton invariant mass has been observed and no radiative corrections are required. This means that in this scenario one can still afford a stop mass as small as 350 GeV or so and couplings λ_T and λ_S can be small ($\sim 10^{-4}$) as well. This is illustrated in figure (1) where, the lightest Higgs boson mass is shown as a function of v_S for $f = 1.5$, $\tan\beta = 4$ and for a set of other parameter choices discussed later. One can see that for a very small v_S ($\lesssim 10^{-3}$ GeV) the tree level Higgs boson mass is 150 GeV and is reduced to 125 GeV for a $v_S \sim 0.2$ GeV. As v_S increases further, $(M_h)_{\text{Tree}}$ starts decreasing rapidly and the Higgs boson mass becomes lighter than 100 GeV. In such a case one requires larger radiative corrections to the Higgs boson mass and this can be achieved with the help of large triplet/singlet couplings ($\mathcal{O}(1)$) and/or large stop mass. For example, with a choice of $\lambda_S = 0.91$ and $\lambda_T = 0.5$, the one-loop radiative corrections to the Higgs boson mass arising from these two couplings are sizable³. In this case, in order to have a 125 GeV Higgs boson, the tree level contribution should be smaller and for a very small v_S ($\sim 10^{-4}$ GeV) and large f ($\gtrsim 1$), this can be achieved with a larger $\tan\beta$. The one loop corrections from the stop loop must also be small and this is realized for small $m_{\tilde{t}}$ and large $\tan\beta$. This is illustrated in figure (2) where we plot mass-contours for the lightest Higgs boson with a mass of 125 GeV in the $m_{\tilde{t}} - \tan\beta$ plane for different choices of f and v_S . One can see from this figure the effect of a larger v_S , which requires a larger stop loop contribution to have a Higgs boson mass of 125 GeV.

4 The fermionic sector

The fermionic sector of the scenario, involving the neutralinos and the charginos, has rich new features. In the context of the present study, when analyzed in conjunction with the scalar sector of the scenario, this sector plays a pivotal role by presenting the defining issues for the phenomenology of this scenario. Its influence ranges over physics of the Higgs boson at current experiments and the physics of the neutrinos before finally reaching out to the domain of astrophysics and cosmology by offering a possible warm dark matter candidate whose actual presence may find support in the recent observations of a satellite-borne X-ray experiment. Thus, it is of crucial importance to study the structure and the content of this sector in appropriate detail.

A thorough discussion of $\mu_{\gamma\gamma}$ in the present scenario requires a study of the masses and the mixing angles of the neutralinos and the charginos. One of the natural consequences of such a $U(1)_R$ -lepton number model with a right-handed neutrino is that one of the left-handed neutrinos (the electron-type one) and the right-handed neutrino become parts of the extended neutralino mass matrix. The electron-type neutrino of the SM can be identified with the lightest neutralino eigenstate. We also address the issue of tree level neutrino mass. Subsequently, we show that in certain region of the parameter space the lightest neutralino-like state can be very light (with a mass of order 100 MeV). This may contribute to the invisible decay width of the lightest Higgs boson. We study the validity

³These choices of λ_T and λ_S are not completely independent. Rather they follow a relationship derived from the requirement of small tree level mass of the active neutrino. This will be discussed in the next section.

of the parameter space when it is subject to the constraint from invisible decay width of the Higgs boson.

4.1 The neutralino sector: R-conserving case

In the neutral fermion sector we have mixing among the Dirac gauginos, the higgsinos, the active neutrino of flavor ‘ a ’ (i.e., ν_e) and the single right-handed neutrino N^c once the electroweak symmetry is broken. The part of the Lagrangian that corresponds to the neutral fermion mass matrix is given by $\mathcal{L} = (\psi^{0+})^T M_\chi^D (\psi^{0-})$ where $\psi^{0+} = (\tilde{b}^0, \tilde{w}^0, \tilde{R}_d^0, N^c)$, with R-charges +1 and $\psi^{0-} = (\tilde{S}, \tilde{T}^0, \tilde{H}_u^0, \nu_e)$ with R-charges -1. The neutral fermion mass matrix M_χ^D is given by

$$M_\chi^D = \begin{pmatrix} M_1^D & 0 & \frac{g'v_u}{\sqrt{2}} & -\frac{g'v_a}{\sqrt{2}} \\ 0 & M_2^D & -\frac{gv_u}{\sqrt{2}} & \frac{gv_a}{\sqrt{2}} \\ \lambda_S v_u & \lambda_T v_u & \mu_u + \lambda_S v_S + \lambda_T v_T & 0 \\ M_R & 0 & -fv_a & -fv_u \end{pmatrix}. \quad (4.1)$$

The above matrix can be diagonalized by a biunitary transformation involving two unitary matrices V^N and U^N and results in four Dirac mass eigenstates $\tilde{\chi}_i^{0+} \equiv \begin{pmatrix} \tilde{\psi}_i^{0+} \\ \tilde{\psi}_i^{0-} \end{pmatrix}$, with $i = 1, 2, 3, 4$ and $\tilde{\psi}_i^{0+} = V_{ij}^N \psi_j^{0+}$, $\tilde{\psi}_i^{0-} = U_{ij}^N \psi_j^{0-}$. The lightest mass eigenstate $\tilde{\chi}_4^{0+}$ is identified with the light Dirac neutrino. The other two active neutrinos remain massless in this case. Generically the Dirac neutrino mass can be in the range of a few eV to tens of MeV. However, one can also accommodate a mass of 0.1 eV or smaller for the Dirac neutrino by assuming certain relationships involving different parameters [88], which are

$$\lambda_T = \lambda_S \tan \theta_W \quad (4.2)$$

and

$$M_R = \frac{\sqrt{2}fM_1^D \tan \beta}{g \tan \theta_W}. \quad (4.3)$$

With these choices the Dirac mass of the neutrino can be written as

$$m_{\nu_e}^D = \frac{v^3 f g \sin \beta}{\sqrt{2}\gamma M_1^D M_2^D} \lambda_T (M_2^D - M_1^D). \quad (4.4)$$

where $\gamma = \mu_u + \lambda_S v_S + \lambda_T v_T$. It is straightforward to check from eq. (4.4) that by suitable choices of the parameters f , λ_T and $\epsilon \equiv (M_2^D - M_1^D)$, one can have a Dirac neutrino mass in the right ballpark of $\lesssim 0.1$ eV. Note that a choice of large $f \sim \mathcal{O}(1)$ is possible for a small λ_T ($\sim 10^{-6}$) and nearly degenerate Dirac gauginos ($\epsilon \lesssim 10^{-1}$) assuming μ_u , M_2^D , M_1^D in the few hundred GeV range.

4.2 The neutralino sector: R-breaking case

R-symmetry is not an exact symmetry and is broken by a small gravitino mass. One can therefore consider the gravitino mass as the order parameter of R-breaking. The breaking

of R-symmetry has to be communicated to the visible sector and in this work we consider anomaly mediation of supersymmetry breaking playing the role of the messenger of R-breaking. This is known as anomaly mediated R-breaking (AMRB) [79]. A non-zero gravitino mass generates Majorana gaugino masses and trilinear scalar couplings. We shall consider the R-breaking effects to be small thus limiting the gravitino mass ($m_{3/2}$) around 10 GeV.

The R-breaking Lagrangian contains the following terms

$$\begin{aligned} \mathcal{L} = & M_1 \tilde{b}^0 \tilde{b}^0 + M_2 \tilde{w}^0 \tilde{w}^0 + M_3 \tilde{g} \tilde{g} + \sum_{b=2,3} A_b^l \tilde{L}_a \tilde{L}_b \tilde{E}_b^c + \sum_{k=1,2,3} A_k^d \tilde{L}_a \tilde{Q}_k \tilde{D}_k^c + \sum_{k=1,2,3} \frac{1}{2} A_{23k}^\lambda \tilde{L}_2 \tilde{L}_3 \tilde{E}_k^c \\ & + \sum_{j,k=1,2,3; b=2,3} A_{bjk}^{\lambda'} \tilde{L}_b \tilde{Q}_j \tilde{D}_k^c + A^\nu H_u \tilde{L}_a \tilde{N}^c + H_u \tilde{Q} A^u \tilde{U}^c \end{aligned} \quad (4.5)$$

where M_1 , M_2 and M_3 are the Majorana mass parameters corresponding to $U(1)$, $SU(2)$ and $SU(3)$ gauginos, respectively and A 's are the scalar trilinear couplings.

The (Majorana) neutralino mass matrix containing R-breaking effects can be written in the basis $\psi^0 = (\tilde{b}^0, \tilde{S}, \tilde{w}^0, \tilde{T}, \tilde{R}_d, \tilde{H}_u^0, N_c, \nu_e)^T$ as

$$\mathcal{L}_{\tilde{\chi}^0}^{\text{mass}} = \frac{1}{2} (\psi^0)^T M_\chi^M \psi^0 + h.c. \quad (4.6)$$

where the symmetric (8×8) neutralino mass matrix M_χ^M is given by

$$M_\chi^M = \begin{pmatrix} M_1 & M_1^D & 0 & 0 & 0 & \frac{g'v_u}{\sqrt{2}} & 0 & -\frac{g'v_a}{\sqrt{2}} \\ M_1^D & 0 & 0 & 0 & \lambda_S v_u & 0 & M_R & 0 \\ 0 & 0 & M_2 & M_2^D & 0 & -\frac{gv_u}{\sqrt{2}} & 0 & \frac{gv_a}{\sqrt{2}} \\ 0 & 0 & M_2^D & 0 & \lambda_T v_u & 0 & 0 & 0 \\ 0 & \lambda_S v_u & 0 & \lambda_T v_u & 0 & \mu_u + \lambda_S v_S + \lambda_T v_T & 0 & 0 \\ \frac{g'v_u}{\sqrt{2}} & 0 & -\frac{gv_u}{\sqrt{2}} & 0 & \mu_u + \lambda_S v_S + \lambda_T v_T & 0 & -fv_a & 0 \\ 0 & M_R & 0 & 0 & 0 & -fv_a & 0 & -fv_u \\ -\frac{g'v_a}{\sqrt{2}} & 0 & \frac{gv_a}{\sqrt{2}} & 0 & 0 & 0 & -fv_u & 0 \end{pmatrix}. \quad (4.7)$$

The above mass matrix can be diagonalized by a unitary transformation given by

$$N^* M_\chi^M N^\dagger = (M_\chi)_{\text{diag}}. \quad (4.8)$$

The two-component mass eigenstates are defined by

$$\chi_i^0 = N_{ij} \psi_j^0, \quad i, j = 1, \dots, 8 \quad (4.9)$$

and one can arrange them in Majorana spinors defined by

$$\tilde{\chi}_i^0 = \begin{pmatrix} \chi_i^0 \\ \bar{\chi}_i^0 \end{pmatrix}, \quad i = 1, \dots, 8. \quad (4.10)$$

Similar to the Dirac case, the lightest eigenvalue ($m_{\tilde{\chi}_8^0}$) of this neutralino mass matrix corresponds to the Majorana neutrino mass. Using the expression of M_R in eq. (4.3) and the relation between λ_S and λ_T in eq. (4.2), the active neutrino mass is given by [88],

$$(m_\nu)_{\text{Tree}} = -v^2 \frac{[g\lambda_T v^2 (M_2^D - M_1^D) \sin \beta]^2}{[M_1 \alpha^2 + M_2 \delta^2]} \quad (4.11)$$

where α and δ are defined as

$$\begin{aligned} \alpha &= \frac{2M_1^D M_2^D \gamma \tan \beta}{g \tan \theta_w} + \sqrt{2} v^2 \lambda_S \tan \beta (M_1^D \sin^2 \beta + M_2^D \cos^2 \beta), \\ \delta &= \sqrt{2} M_1^D v^2 \lambda_T \tan \beta \end{aligned} \quad (4.12)$$

and the quantity γ has been defined earlier in section 4.1. This shows that to have an appropriate neutrino mass we require the Dirac gaugino masses to be highly degenerate. The requirement on the degree of degeneracy can be somewhat relaxed if one chooses an appropriately small value of λ_T . Such a choice, in turn, would imply an almost negligible radiative contribution to the lightest Higgs boson mass. Interestingly, the Yukawa coupling does not appear in the expression for $(m_\nu)_{\text{Tree}}$ in eq. (4.11). This is precisely because of the relation between M_R and f in eq. (4.3). However, ‘ f ’ has some interesting effects on the next-to-lightest eigenstates of the mass matrix. The following situations are phenomenologically important:

- A large value of $f \sim \mathcal{O}(1)$ generates a very light bino-like neutralino ($\tilde{\chi}_7^0$) with mass around a few hundred MeV. In this case, this is the lightest supersymmetric particle (LSP) and its mass is mainly controlled by the R-breaking Majorana gaugino mass parameter M_1 . A very light neutralino has profound consequences in both cosmology as well as in collider physics [100–109]. In the context of the present model one can easily satisfy the stringent constraint coming from the invisible decay width of the Z boson because the light neutralino is predominantly a bino. One should also take into account the constraints coming from the invisible decay branching ratio of the lightest Higgs boson. In our scenario $h \rightarrow \tilde{\chi}_7^0 \tilde{\chi}_8^0$ (where $\tilde{\chi}_8^0$ is the light active neutrino) could effectively contribute to the invisible final state. This is because, although $\tilde{\chi}_7^0$ would undergo an R-parity violating decay, for example, $\tilde{\chi}_7^0 \rightarrow e^+ e^- \nu$, the resulting four body final state presumably has to be dealt with as an invisible mode for the lightest Higgs boson. Such constraints are discussed in detail later in this paper. Note that $\Gamma(h \rightarrow \tilde{\chi}_7^0 \tilde{\chi}_7^0)$ is negligibly small because of suppressed $h\text{-}\tilde{\chi}_7^0\text{-}\tilde{\chi}_7^0$ coupling for a bino-dominated, $\tilde{\chi}_7^0$.

A 10 GeV gravitino NLSP could also decay to a final state comprising of the lightest neutralino accompanied by a photon. In order to avoid the strong constraint on such a decay process coming from big-bang nucleosynthesis (BBN) one must consider an upper bound on the reheating temperature of the universe $T_R \lesssim 10^6$ GeV [104, 111]. In addition, such a light state is subjected to various collider bounds [100] and bounds coming from rare meson decays such as the decays of pseudo-scalar and vector mesons into light neutralino should also be investigated [105] in this context. The spectra of

low lying mass eigenstates for the large f case will be shown later for a few benchmark points.

- For small $f \sim \mathcal{O}(10^{-4})$, $\tilde{\chi}_7^0$ is a sterile neutrino state, which is a plausible warm dark matter candidate with appropriate relic density. Its mass can be approximated from the 8×8 neutralino mass matrix as follows:

$$M_N^R \approx M_1 \frac{2f^2 \tan^2 \beta}{g'^2}. \quad (4.13)$$

For a wide range of parameters, the active-sterile mixing angle, denoted as θ_{14} , can be estimated as

$$\theta_{14}^2 = \frac{(m_\nu)_{Tree}}{M_N^R}. \quad (4.14)$$

Furthermore, the sterile neutrino can be identified with a warm dark matter candidate only if the following requirements are fulfilled. These are: (i) it should be heavier than 0.4 keV, which is the bound obtained from a model independent analysis [112] and (ii) the active-sterile mixing needs to be small enough to satisfy the stringent constraint coming from different X-ray experiments [113].

Under the circumstances, the lightest neutralino-like state is the next-to-next-to-lightest eigenstate ($\tilde{\chi}_6^0$) of the neutralino mass matrix. Its composition is mainly controlled by the parameter μ_u , chosen to be rather close to the electroweak scale ($M_1^D, M_2^D > \mu_u$). The masses of the lighter neutralino states for this case (small f) will be presented later.

4.3 The chargino sector

We shall now discuss the chargino sector in some detail as it plays a crucial role in the decay $h \rightarrow \gamma\gamma$. The relevant Lagrangian after R-breaking in the AMRB scenario obtains the following form:

$$\begin{aligned} \mathcal{L}_{ch} = & M_2 \tilde{w}^+ \tilde{w}^- + M_2^D \tilde{T}_u^+ \tilde{w}^- + \sqrt{2} \lambda_T v_u \tilde{T}_u^+ \tilde{R}_d^- + g v_u \tilde{H}_u^+ \tilde{w}^- - \mu_u \tilde{H}_u^+ \tilde{R}_d^- + \lambda_T v_T \tilde{H}_u^+ \tilde{R}_d^- \\ & - \lambda_S v_S \tilde{H}_u^+ \tilde{R}_d^- + g v_a \tilde{w}^+ e_L^- + M_2^D \tilde{T}_u^+ \tilde{w}^- + m_e e_R^c e_L^- + h.c. \end{aligned} \quad (4.15)$$

The chargino mass matrix, in the basis $(\tilde{w}^+, \tilde{T}_u^+, \tilde{H}_u^+, e_R^c)$ and $(\tilde{w}^-, \tilde{T}_d^-, \tilde{R}_d^-, e_L^-)$, is written as

$$M_c = \begin{pmatrix} M_2 & M_2^D & 0 & g v_a \\ M_2^D & 0 & \sqrt{2} v_u \lambda_T & 0 \\ g v_u & 0 & -\mu_u - \lambda_S v_S + \lambda_T v_T & 0 \\ 0 & 0 & 0 & m_e \end{pmatrix}. \quad (4.16)$$

This matrix can be diagonalized by a biunitary transformation, $U M_c V^T = M_D^\pm$. The chargino mass eigenstates are related to the gauge eigenstates by these two matrices U and V . The chargino mass eigenstates (two-component) are written in a compact form as

$$\begin{aligned} \chi_i^- &= U_{ij} \psi_j^-, \\ \chi_i^+ &= V_{ij} \psi_j^+, \end{aligned} \quad (4.17)$$

where

$$\psi_i^+ = \begin{pmatrix} \tilde{w}^+ \\ \tilde{T}_u^+ \\ \tilde{H}_u^+ \\ e_R^c \end{pmatrix}, \quad \psi_i^- = \begin{pmatrix} \tilde{w}^- \\ \tilde{T}_d^- \\ \tilde{R}_d^- \\ e_L^- \end{pmatrix}. \quad (4.18)$$

The four-component Dirac spinors can be written in terms of these two-component spinors as

$$\tilde{\chi}_i^+ = \begin{pmatrix} \chi_i^+ \\ \bar{\chi}_i^- \end{pmatrix}, \quad (i = 1, \dots, 4). \quad (4.19)$$

It is to be noted that $\tilde{\chi}_i^c \equiv (\tilde{\chi}_i^+)^c = \tilde{\chi}_i^-$ is a negatively charged chargino. Hence, the lightest chargino ($\tilde{\chi}_4^-$) corresponds to the electron and the structure of the chargino mass matrix ensures (see eq. 4.16) that the lightest mass eigenvalue remains unaltered from the input mass parameter for the electron, i.e., $m_e = 0.5$ MeV.

Let us now analyze the composition of different chargino states and how they affect the decay width $\Gamma(h \rightarrow \gamma\gamma)$ in this model. Due to constraints from the electroweak precision measurements one must consider a heavy Dirac wino mass [84]. Furthermore, a small tree level Majorana neutrino mass demands a mass-degeneracy of the electroweak Dirac gauginos as is obvious from eq. (4.11). In addition, we assume an order one λ_T which we use throughout this work for numerical purposes. With these, we observe the following features of the next-to-lightest physical chargino state which could potentially contribute to $\mu_{\gamma\gamma}$:

- In the limit when $M_2^D \gg \mu_u$, the next-to-lightest chargino, χ_3^- (which is actually the lightest chargino-like state in the MSSM sense), comprises mainly of \tilde{R}_d^- with a very little admixture of \tilde{T}_d^- while χ_3^+ is dominated by \tilde{H}_u^+ with a small admixture of \tilde{w}^+ .
- For $M_2^D \ll \mu_u$, χ_3^- is predominantly \tilde{w}^- while χ_3^+ is composed mainly of \tilde{T}_u^+ .
- Finally, for $M_2^D \approx \mu_u$, χ_3^- is dominantly \tilde{w}^- and χ_3^+ is mostly made up of \tilde{T}_u^+ .

Apart from the electron, the mass of the chargino states are controlled mainly by the parameters M_2^D and μ . We have varied the input parameters in such a way that the lightest chargino-like state is always heavier than 104 GeV [110]. The chargino mass spectra corresponding to different benchmark points will be presented later.

5 Contributions to $\mu_{\gamma\gamma}$

The resonant production of the Higgs boson at the LHC, with the dominant contribution coming from gluon fusion, is related to its decay to gluons by $\hat{\sigma}(gg \rightarrow h) = \pi^2 \Gamma(h \rightarrow$

$gg)/8m_h^3$. Thus, $\mu_{\gamma\gamma}$ can be expressed entirely in terms of various decay widths of the Higgs boson as follows [23, 24]:

$$\begin{aligned}\mu_{\gamma\gamma} &= \frac{\sigma(pp \rightarrow h \rightarrow \gamma\gamma)}{\sigma(pp \rightarrow h \rightarrow \gamma\gamma)^{\text{SM}}}, \\ &= \frac{\Gamma(h \rightarrow gg)}{\Gamma(h \rightarrow gg)^{\text{SM}}}, \frac{\Gamma_{\text{TOT}}^{\text{SM}}}{\Gamma_{\text{TOT}}}, \frac{\Gamma(h \rightarrow \gamma\gamma)}{\Gamma(h \rightarrow \gamma\gamma)^{\text{SM}}}, \\ &= k_{gg} \cdot k_{\text{TOT}}^{-1} \cdot k_{\gamma\gamma},\end{aligned}\tag{5.1}$$

where we use $k_{gg} \equiv \frac{\hat{\sigma}(gg \rightarrow h)}{\hat{\sigma}(gg \rightarrow h)^{\text{SM}}} = \frac{\Gamma(h \rightarrow gg)}{\Gamma(h \rightarrow gg)^{\text{SM}}}$ and $k_{\text{TOT}} = \frac{\Gamma_{\text{TOT}}}{\Gamma_{\text{TOT}}^{\text{SM}}}$, Γ_{TOT} being the total decay width of the Higgs boson in the present scenario. The decay of $h \rightarrow \gamma\gamma$ is mediated mainly by the top quark and the W^\pm -loops in the SM and in addition, by top squark, charged Higgs and chargino loops in our scenario. In the subsequent discussion we investigate these widths in some detail.

As discussed before, note that in this model we have integrated out the down type Higgs (\widehat{H}_d) superfield and the sneutrino $\tilde{\nu}_a$ ($a = 1(e)$) plays the role of the down type Higgs boson acquiring a large non-zero vev . The sneutrino ($\tilde{\nu}_a$) couples to charged leptons (second and third generation) and down type quarks via R -parity violating couplings which are identified with the standard Yukawa couplings. Thus, the couplings of the Higgs boson to charged leptons and quarks remain the same as in the MSSM. This is apparent from the first term given in eq. (2.7).

5.1 The decay $h \rightarrow gg$

The partial width of the Higgs boson decaying to a pair of gluons via loops involving quarks and squarks is given by

$$\Gamma(h \rightarrow gg) = \frac{G_F \alpha_s^2 m_h^3}{36\sqrt{2}\pi^3} \left| \sum_Q g_Q^h A_Q^h(\tau_Q) + \sum_{\tilde{Q}} g_{\tilde{Q}}^h A_{\tilde{Q}}^h(\tau_{\tilde{Q}}) \right|^2,\tag{5.2}$$

where $\tau_i = m_h^2/4m_i^2$, G_F is the Fermi constant, α_s is the strong coupling constant and

$$\begin{aligned}A_Q^h(\tau) &= \frac{3}{2} [\tau + (\tau - 1)f(\tau)] / \tau^2, \\ A_{\tilde{Q}}^h(\tau) &= -\frac{3}{4} [\tau - f(\tau)] / \tau^2,\end{aligned}\tag{5.3}$$

with $f(\tau)$ given by

$$f(\tau) = \begin{cases} \arcsin^2 \sqrt{\tau} & \tau \leq 1, \\ -\frac{1}{4} \left[\log \frac{1 + \sqrt{1 - \tau^{-1}}}{1 - \sqrt{1 - \tau^{-1}}} - i\pi \right]^2 & \tau > 1. \end{cases}\tag{5.4}$$

The couplings are given by

$$\begin{aligned}
g_Q^h(u) &= \frac{\cos \alpha}{\sin \beta}, \\
g_Q^h(d) &= -\frac{\sin \alpha}{\cos \beta}, \\
g_{\tilde{Q}}^h &= \frac{m_f^2}{m_{\tilde{Q}}^2} g_Q^h \mp \frac{m_Z^2}{m_{\tilde{Q}}^2} (I_3^f - e_f \sin^2 \theta_W) \sin(\alpha + \beta),
\end{aligned} \tag{5.5}$$

where the angle α is defined in eq. (3.11) and $\tan \beta = v_u/v_d$. The couplings of the Higgs boson with the left- and the right-handed squarks are exactly the same as in the MSSM. However, one can neglect the mixing between the left- and the right-handed squarks due to the absence of the μ -term and the A -terms⁴.

As far as the production of the Higgs boson is concerned, we shall show later that a rather light top squark with mass around 200–300 GeV enhances the value of k_{gg} compared to the SM. The SM and the MSSM results for the decay $h \rightarrow gg$ can be found in [114–116].

5.2 The decay $h \rightarrow \gamma\gamma$

In the SM, the primary contribution to the decay $h \rightarrow \gamma\gamma$ comes from the W boson loop and the top quark loop with the former playing the dominant role. In supersymmetric models, the charged Higgs (H^\pm), top squark (\tilde{t}) and the chargino ($\tilde{\chi}^\pm$) provide extra contributions in addition to the W boson and the top quark loop. The authors of ref. [24] have noted that the relative strengths of the loop contributions involving the vector bosons, the fermions and the scalars with mass around 100 GeV follow a rough ratio of 8 : 1.5 : 0.4. Nonetheless, a light charged Higgs boson (H^\pm) could contribute substantially if one considers a large hH^+H^- coupling. However, since the triplet vev is small, the contribution of the triplet to the charged Higgs state is negligible. On the other hand, charginos in loop could enhance the $h \rightarrow \gamma\gamma$ decay width, in particular, when they are light and/or diagrams involving them interfere constructively with the W -mediated loop diagram.

The Higgs to diphoton decay rate can be written down as [114]

$$\begin{aligned}
\Gamma(h \rightarrow \gamma\gamma) &= \frac{G_F \alpha^2 m_h^3}{128 \sqrt{2} \pi^3} \left| \sum_f N_c Q_f^2 g_f^h A_{1/2}^h + g_{hW^+W^-} A_1^h + g_{hH^+H^-} A_0^h + \sum_{\tilde{c}} g_{h\tilde{\chi}_i^+ \tilde{\chi}_j^-} A_{1/2}^h \right. \\
&\quad \left. + \sum_{\tilde{f}} N_c e_{\tilde{f}}^2 g_{h\tilde{f}\tilde{f}} A_0^h \right|^2,
\end{aligned} \tag{5.6}$$

where

$$\begin{aligned}
A_1^h &= -[2\tau^2 + 3\tau + 3(2\tau - 1)f(\tau)]/\tau^2, \\
A_{1/2}^h &= 2[\tau + (\tau - 1)f(\tau)]/\tau^2, \\
A_0^h &= -[\tau - f(\tau)]/\tau^2,
\end{aligned} \tag{5.7}$$

⁴Actually, tiny ‘ A ’-terms are generated because of the breaking of R -symmetry but we can neglect them in the present context.

with the loop functions already defined in eq. (5.4). The relevant couplings are given by,

$$\begin{aligned}
g_{h\bar{u}u} &= \frac{\cos \alpha}{\sin \beta}, \\
g_{h\bar{d}d} &= -\frac{\sin \alpha}{\cos \beta}, \\
g_{hWW} &= \sin(\beta - \alpha), \\
g_{hH^+H^-} &= \frac{m_W^2}{m_{H^\pm}^2} \left[\sin(\beta - \alpha) + \frac{\cos 2\beta \sin(\beta + \alpha)}{2 \cos^2 \theta_W} \right], \\
g_{h\tilde{f}\tilde{f}} &= \frac{m_f^2}{m_{\tilde{f}}^2} g_{hff} \mp \frac{m_Z^2}{m_{\tilde{f}}^2} [I_3^f - e_f \sin^2 \theta_w] \sin(\alpha + \beta), \\
g_{h\tilde{\chi}_i^+ \tilde{\chi}_j^-} &= 2 \frac{m_W}{m_{\tilde{c}_k}} (\xi_{ij} \sin \alpha - \eta_{ij} \cos \alpha).
\end{aligned} \tag{5.8}$$

Here $\xi_{ij} = -\frac{1}{\sqrt{2}} V_{i1} U_{j4}$ and $\eta_{ij} = -\frac{1}{\sqrt{2}} \left(\frac{\sqrt{2} \lambda_T}{g} U_{i3} V_{j2} + U_{i1} V_{j3} \right)$. The masses which appear in the denominator of the couplings given above, represent physical masses propagating in the loop. For example, $m_{\tilde{c}_k}$ are the physical chargino masses, $m_{\tilde{f}}$ are the physical masses of the sfermions and so on. We present the complete set of Higgs-chargino-chargino interaction vertices in Appendix A⁵.

As noted earlier, the largest contribution in the Higgs decay rate to two photons comes from the W boson loop. Similar to the MSSM, the hWW coupling gets modified by the factor $\sin(\beta - \alpha)$. Hence, in order to have a significant contribution from the W boson loop in our model, the angles α and β need to be aligned in such a way that one obtains a large value of $\sin(\beta - \alpha)$, which can be achieved in the decoupling regime, i.e., the coupling to the lightest Higgs boson becomes SM like.

In fig. 3, we illustrate the variations of the couplings $g_{hW^+W^-}$ and $g_{h\tilde{\chi}_3^+ \tilde{\chi}_3^-}$, which might play important roles in the decay $h \rightarrow \gamma\gamma$. We choose $M_1^D = 1.5$ TeV, $\mu_u = 200$ GeV, $m_{3/2} = 10$ GeV, $m_{\tilde{t}} = 500$ GeV, $v_S = 10^{-4}$ GeV, $v_T = 10^{-3}$ GeV and retain a near degeneracy between the Dirac gaugino masses with $\epsilon \equiv (M_2^D - M_1^D) = 10^{-1}$ GeV, with $f = 0.8$ and $B\mu_L = -(400)^2 (\text{GeV})^2$. From the left panel of fig. 3 we observe that the hWW coupling is almost SM like as we are essentially working in the decoupling limit. This implies that the W -loop contribution in the $h \rightarrow \gamma\gamma$ process remains almost unchanged with varying $\tan \beta$. On the other hand, as $\mu_u \ll M_{1,2}^D$, the next-to-lightest chargino state is dominantly controlled by the μ_u parameter. For this case, the coupling $g_{h\tilde{\chi}_3^+ \tilde{\chi}_3^-}$ is plotted as a function of $\tan \beta$ in the right panel of fig. 3. One can clearly see that $g_{h\tilde{\chi}_3^+ \tilde{\chi}_3^-}$ is already much suppressed compared to $g_{hW^+W^-}$, for the entire range of $\tan \beta$. From the expression for $g_{h\tilde{\chi}_3^+ \tilde{\chi}_3^-}$ in eq. (5.8) it is straightforward to verify that this coupling remains very much suppressed for all the different cases mentioned in section 4.3. The Higgs boson couplings to heavier charginos are also highly suppressed as can be seen from fig. 4. Thus, the contribution of charginos in $\Gamma(h \rightarrow \gamma\gamma)$ would, in any case, be insignificant. Referring back to eq. (5.1), we are now in a position to have some quantitative estimates of the quantities k_{gg} and $k_{\gamma\gamma}$ which control the signal strength $\mu_{\gamma\gamma}$. In fig. 5 we illustrate their variations

⁵For the MSSM case see refs. [116, 117].

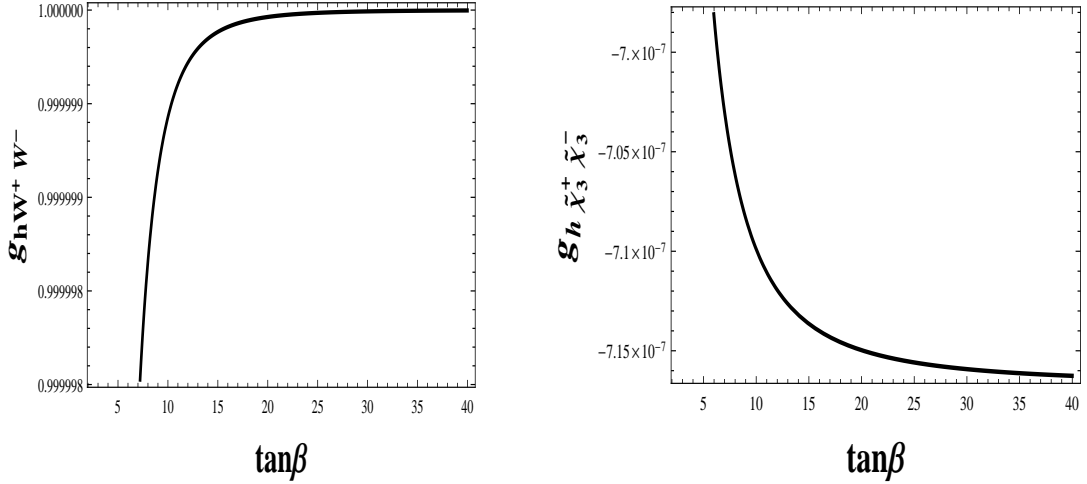


Figure 3. Couplings of the lightest Higgs boson to a pair of W -bosons (left) and to a pair of light charginos ($\tilde{\chi}_3^\pm$) (right).

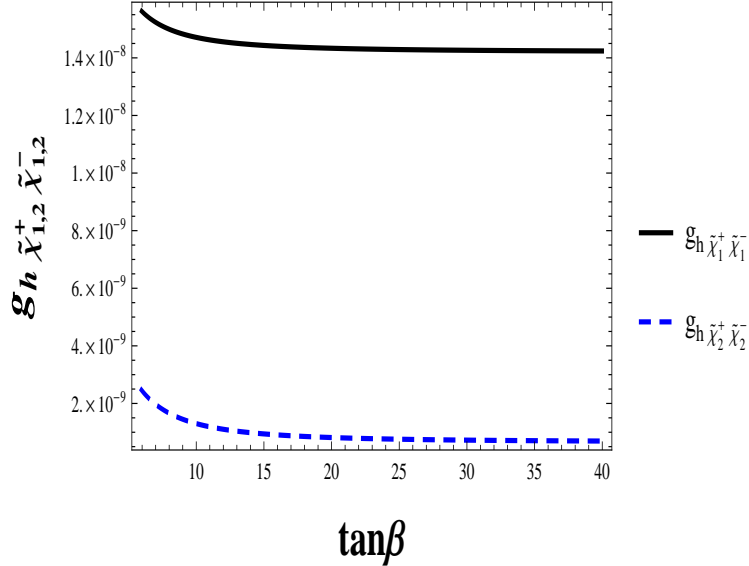


Figure 4. Couplings of the Higgs boson to heavier charginos. The thick black line represents the coupling to the heaviest chargino ($\tilde{\chi}_1^\pm$) whereas the blue dashed one represents the same to the chargino immediately lighter to it ($\tilde{\chi}_2^\pm$).

(k_{gg} in red and $k_{\gamma\gamma}$ in blue) as functions of the mass of the top squark for various values of $\tan\beta$. We observe that k_{gg} is not at all sensitive to $\tan\beta$ (all three curves in red for three $\tan\beta$ values are found to be overlapping). This is since we considered $gg \rightarrow h$ production via loops involving the top quark and the top squark. The couplings involved there carry a factor $\cos\alpha/\sin\beta$, which varies only marginally with respect to $\tan\beta$. Similarly $k_{\gamma\gamma}$ also remains insensitive with $\tan\beta$. The reason being, $\Gamma(h \rightarrow \gamma\gamma)$ receives major contribution from the W boson induced loop where the involved coupling goes as $\sin(\beta - \alpha)$. As shown

vividly in the left panel of fig. 3 that hWW coupling remains almost unchanged with $\tan\beta$. As a result, $k_{\gamma\gamma}$ shares the same feature as k_{gg} as far as variation with respect to $\tan\beta$ is concerned.

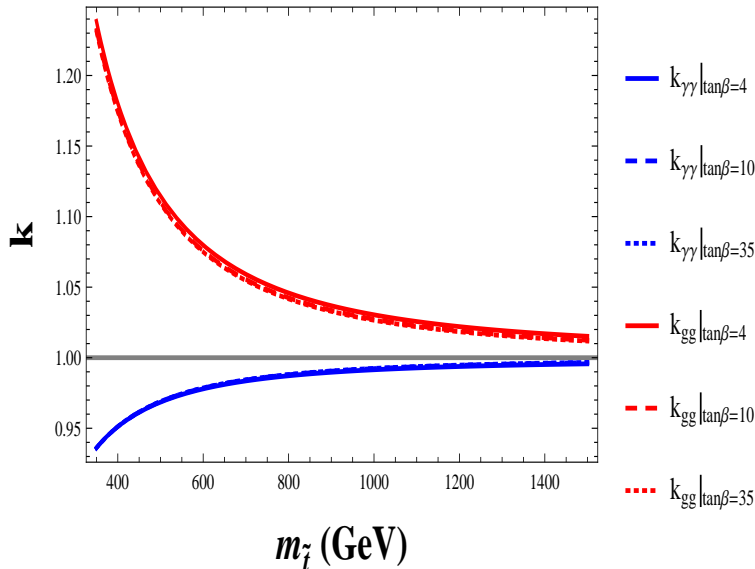


Figure 5. Variations of k_{gg} (in red) and $k_{\gamma\gamma}$ (in blue) as functions of $M_{\tilde{t}}$ for $\tan\beta = 4, 10, 35$.

It is observed that for light top squarks, k_{gg} gets enhanced by a considerable amount. However, in that very region, $k_{\gamma\gamma}$ is rather small for small $\tan\beta$, and it becomes somewhat larger for higher $\tan\beta$. However, it is found that $k_{gg} > 1$ while $k_{\gamma\gamma} < 1$, all through. We have also checked that the illustrated variations of k_{gg} and $k_{\gamma\gamma}$ are following their respective gross trends in the MSSM closely in the limit of zero left-right mixing in the scalar sector. Note that for this plot we have not incorporated the constraints from the mass of the Higgs boson and the requirement of having no tachyonic scalar states. In section 6, while discussing the quantitative impact of the recent LHC results on such a scenario, we present results of detailed scan of the parameter space by including all these constraints.

All the previous plots consider a large values of ‘ f ’ ($f \sim \mathcal{O}(1)$) for which one obtains a large tree level correction to the Higgs boson mass as well as an appropriate mass for the active neutrino at the tree level. We adopt such a scenario with relatively large values of ‘ f ’ in our study of the Higgs boson decay rates which we present in the next subsection.

5.3 Higgs boson decaying to charginos and neutralinos

In the presence of much lighter charginos and neutralinos (as discussed in sections 4.2 and 4.3), an SM-like Higgs boson with mass around 125 GeV could undergo decays to a pair of these states. We study these things in detail in this section.

It has been noted in section 4.2, that the smallest eigenvalue ($m_{\tilde{\chi}_8^0}$) of the neutralino mass matrix corresponds to the neutrino mass. The next-to-lightest neutralino ($\tilde{\chi}_7^0$) turns out to be a bino-like neutralino (the sterile neutrino) for large (small) values of ‘ f ’. More-

over, the mass of the next-to-next-to-lightest neutralino state ($\tilde{\chi}_6^0$) is mostly controlled by μ_u . Since we have chosen μ_u to be very close to the electroweak scale, the Higgs boson decay to a pair of $\tilde{\chi}_6^0$ is not possible. The presence of light neutralino states may enhance the invisible decay width of the Higgs boson considerably. Amongst them, the most dominant contribution comes from $h\text{-}\tilde{\chi}_7^0\text{-}\tilde{\chi}_8^0$ coupling. However, a detailed study reveals that the contribution of this coupling is not substantial and hence the corresponding decay width is rather small. It is clear from fig. 6 that the $h\text{-}\tilde{\chi}_7^0\text{-}\tilde{\chi}_8^0$ coupling grows for small $\tan\beta$. This

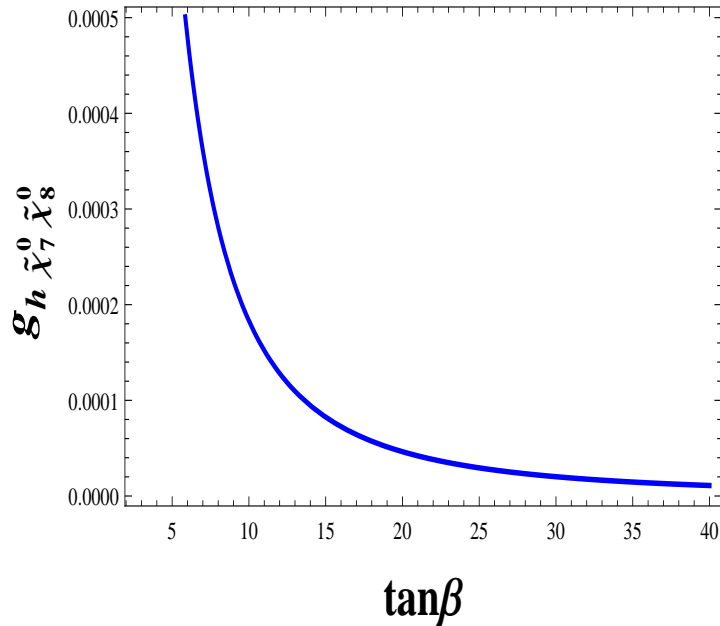


Figure 6. Variation of the $h - \tilde{\chi}_7^0 - \tilde{\chi}_8^0$ coupling as a function of $\tan\beta$.

is essentially because for smaller values of $\tan\beta$, the sneutrino component of the lightest Higgs boson mass eigenstate is large, which results in a slightly larger value of this coupling. This fact also shows up for the invisible decay widths of the Higgs boson, which we will discuss later.

On the other hand, the lightest chargino eigenstate ($\tilde{\chi}_4^\pm$) corresponds to the electron. The mass of the next-to-lightest chargino ($\tilde{\chi}_3^\pm$) is again controlled by μ_u if $\mu_u < M_2^D$. Thus, decay of the Higgs boson to a pair of $\tilde{\chi}_3^\pm$ is not possible. The most general expressions for the partial widths of the Higgs boson decaying to a pair of neutralinos ($\Gamma(h \rightarrow \tilde{\chi}_i^0 \tilde{\chi}_j^0)$) or a pair of charginos ($\Gamma(h \rightarrow \tilde{\chi}_i^+ \tilde{\chi}_j^-)$) can be found in the Appendix A and B.

5.4 The total decay width of the Higgs boson

In this section we collect the partial decay widths of the lightest Higgs boson that dominantly contribute to its total decay width. The latter is thus given by⁶

$$\begin{aligned}\Gamma_{\text{TOT}} = & \Gamma(h \rightarrow b\bar{b}) + \Gamma(h \rightarrow \tau\bar{\tau}) + \Gamma(h \rightarrow gg) + \Gamma(h \rightarrow WW^*) + \Gamma(h \rightarrow ZZ^*) \\ & + \Gamma(h \rightarrow \gamma\gamma) + \Gamma(h \rightarrow \tilde{\chi}_i^0 \tilde{\chi}_j^0) + \Gamma(h \rightarrow \tilde{\chi}_i^+ \tilde{\chi}_j^-).\end{aligned}\tag{5.9}$$

For completeness, we present here the analytical expressions for all the decay rates which go into our analysis but were not presented earlier. These are as follows:

$$\begin{aligned}\Gamma(h \rightarrow b\bar{b}) &= \frac{3G_F m_b^2 m_h}{4\pi\sqrt{2}} \left(\frac{\sin\alpha}{\cos\beta}\right)^2 \left[1 - \frac{4m_b^2}{m_h^2}\right]^{3/2}, \\ \Gamma(h \rightarrow \tau\bar{\tau}) &= \frac{G_F m_\tau^2 m_h}{4\pi\sqrt{2}} \left(\frac{\sin\alpha}{\cos\beta}\right)^2 \left[1 - \frac{4m_\tau^2}{m_h^2}\right]^{3/2}, \\ \Gamma(h \rightarrow WW^*) &= \frac{3G_F^2 m_W^4 m_h}{16\pi^3} \sin^2(\alpha - \beta) R\left(\frac{m_W^2}{m_h^2}\right), \\ \Gamma(h \rightarrow ZZ^*) &= \frac{3G_F^2 m_Z^4 m_h}{16\pi^3} \left[\frac{7}{12} - \frac{10}{9} \sin^2\theta_W + \frac{40}{27} \sin^4\theta_W\right] R\left(\frac{m_Z^2}{m_h^2}\right).\end{aligned}\tag{5.10}$$

The function $R(x)$ is defined as [116, 118, 119]

$$R(x) = 3 \frac{(1 - 8x + 20x^2)}{\sqrt{(4x - 1)} \arccos\left(\frac{3x-1}{2x^{3/2}}\right)} - \left(\frac{1-x}{2x}\right)(2 - 13x + 47x^2) - \frac{3}{2}(1 - 6x + 4x^2) \log x.\tag{5.11}$$

The Higgs boson decay rates to charginos and neutralinos are shown in Appendix A and B respectively. The recent CMS analysis constrains the total decay width of the Higgs boson to be less than 14 MeV or so [120]. In the subsequent sections we present the numerical results of our analysis pertaining to the diphoton signal strength $\mu_{\gamma\gamma}$ and subject this to important experimental findings.

6 Impact of the LHC results

In this section, we discuss the impact of the findings from the LHC pertaining to the Higgs sector on the scenario under discussion. As pointed out earlier, two broad scenarios based on the magnitude of ‘ f ’ worth special attention: the scenario with large ‘ f ’ ($\sim \mathcal{O}(1)$) and the one for which ‘ f ’ is rather small.

6.1 The case of large neutrino Yukawa coupling, $f \sim \mathcal{O}(1)$

A large neutrino Yukawa coupling ($f \sim \mathcal{O}(1)$) already enhances the tree level Higgs boson mass. Thus, such a scenario banks less on large radiative contributions from the top squark

⁶We neglect the rare decay modes like $H \rightarrow Z\gamma, \gamma^*\gamma, \mu^+\mu^-, e^+e^-$ etc.

loops to uplift the same. Further, an appropriately small tree level Majorana neutrino mass (the lightest neutralino) can be obtained along with a light bino-like neutralino ($\tilde{\chi}_7^0$, the next-to-lightest neutralino) once R -symmetry is broken explicitly, via anomaly mediation. The mass of this neutralino is essentially controlled by the R -symmetry breaking Majorana mass term of the $U(1)$ gaugino (the bino), i.e., M_1 , and hence related to the gravitino mass $m_{3/2}$. Since we assume $m_{3/2} \sim 10$ GeV, the next-to-lightest neutralino acquires a mass of the order of a few hundred MeV. The presence of such a light bino like neutralino implies an additional contribution to the total decay width of the Higgs boson. We also looked at the diphoton signal strength $\mu_{\gamma\gamma}$ and compared it with the latest ATLAS and CMS results.

6.1.1 Invisible branching ratio of the Higgs boson

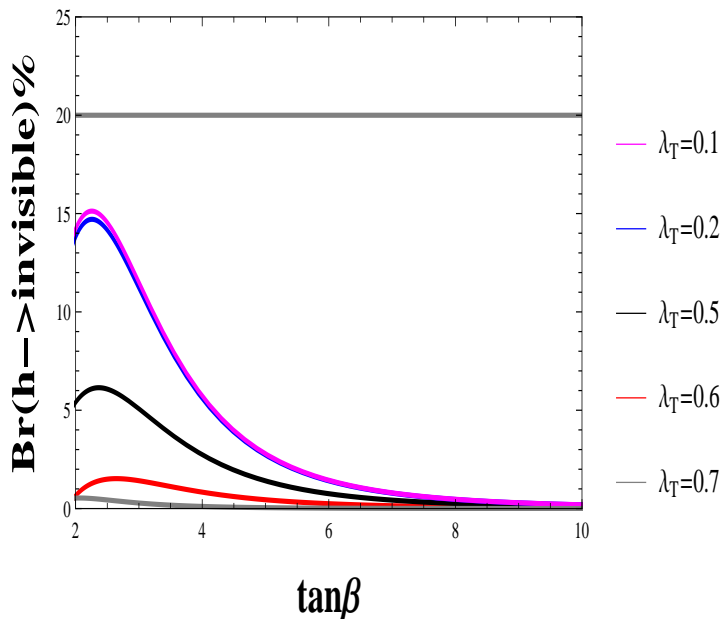


Figure 7. The lightest Higgs boson invisible branching ratio as a function of $\tan\beta$ for different values of λ_T . The horizontal line corresponds to the upper limit on the invisible branching ratio from model independent analysis [121].

To take into account the constraints coming from the invisible decay branching ratio of the lightest Higgs boson we have fixed $M_1^D = M_2^D = 1.5$ TeV, $\mu_u = 200$ GeV, (i.e., $M_1, M_2 \ll \mu_u$), $m_{3/2} = 10$ GeV, $m_{\tilde{t}} = 500$ GeV, $v_S = 10^{-4}$ GeV and $v_T = 10^{-3}$ GeV with $f = 0.8$, $B\mu_L = -(200)^2(\text{GeV})^2$. As discussed earlier, the partial decay width of the Higgs boson decaying to a neutrino and a neutralino ($h \rightarrow \tilde{\chi}_7^0 \tilde{\chi}_8^0$) could essentially contribute to the invisible final state. This can be understood from the fact that although $\tilde{\chi}_7^0$ would undergo R -parity violating decays $\tilde{\chi}_7^0 \rightarrow q\bar{q}\nu$, $e^+e^-\nu$, $\nu\nu\nu$, $q\bar{q}'e^-$, where q, q' are the SM light quark states from the first two generations, these decay modes involve very small couplings and as a result, the decay length happens to be much larger than the collider dimension. Therefore, the LSP neutralino contributes to missing energy (MET) signals

[122]. Note that $\Gamma(h \rightarrow \tilde{\chi}_7^0 \tilde{\chi}_7^0)$ is negligibly small because of suppressed $h\text{-}\tilde{\chi}_7^0\text{-}\tilde{\chi}_7^0$ coupling for a bino-dominated, $\tilde{\chi}_7^0$.

We observe from fig. 7 that this partial decay width is comparatively larger for smaller values of $\tan\beta$ and λ_T . However, it is clear that the presence of a bino-like neutralino state is not yet constrained from the invisible decay mode of the Higgs boson in our scenario with all the curves staying well below the experimentally derived [121] upper bound of $\sim 20\%$ for the invisible branching fraction of the Higgs boson.

6.1.2 The signal strength $\mu_{\gamma\gamma}$

It is now important to analyse the signal strength corresponding to the $h \rightarrow \gamma\gamma$ channel. In fig. 8 we fix $\lambda_T = 0.45$, and $f = 0.8$, with all other parameters held at the values mentioned in section 5.2. The red dashed lines represent the contours of $m_h = 124$ GeV and 126.2 GeV

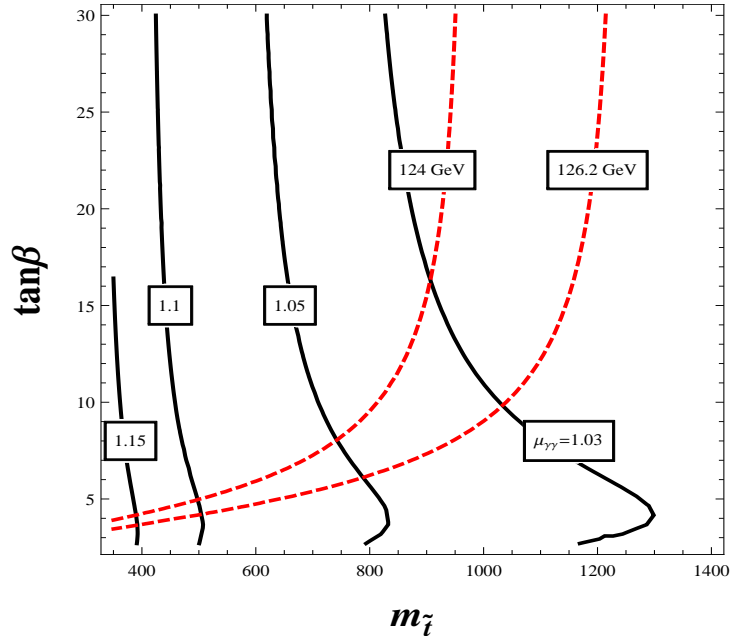


Figure 8. Contours of various fixed values of m_h (124 GeV and 126.2 GeV), $\mu_{\gamma\gamma}$ and k_{TOT} in the $m_{\tilde{t}}\text{-}\tan\beta$ plane. λ_T and f are fixed at 0.45 and 0.8, respectively. Other parameters are set at the values as mentioned in the text.

respectively and enclose the experimentally allowed range of m_h . The black thick lines are the contours of fixed $\mu_{\gamma\gamma}$ with values 1.15, 1.1, 1.05 and 1.03 respectively. Figure 8 shows that there is an available region of parameter space consistent with the latest experimental findings involving m_h and $\mu_{\gamma\gamma}$. Relatively low values of the top squark mass results in an increase of the cross section for the resonant Higgs boson production through gluon fusion and thus enhances $\mu_{\gamma\gamma}$. On the other hand $\mu_{\gamma\gamma}$ is almost insensitive to $\tan\beta$ for $\tan\beta \geq 15$. This is because $hb\bar{b}$ coupling (which controls the total decay width of the Higgs boson in a significant way) becomes independent of $\tan\beta$ for larger values of this parameter.

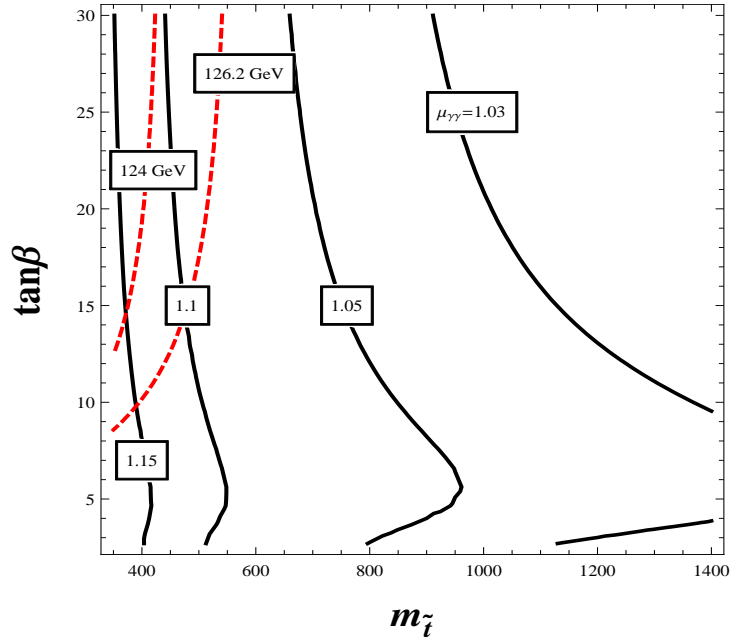


Figure 9. Same as in fig. 8 but with $\lambda_T = 0.5$ and $f = 1$.

Figure 9 addresses the same issue but with $f = 1$ and $\lambda_T = 0.5$. Since a larger value of λ_T already provides a significant contribution to the Higgs boson mass via radiative correction, only light top squarks are compatible with the measured range of m_h . Moreover, a larger value of ‘ f ’ implies a larger $\tan \beta$ to have the Higgs boson mass in the correct range. It is pertinent to mention that these plots use spectra of particles which are consistent with the lower bound on the lightest chargino mass (> 104 GeV, from the LEP experiments) and are also free from tachyonic scalar states.

6.1.3 Relative signal strengths in different final states

In this subsection we briefly discuss how other final states arising from the lightest Higgs boson are expected to be affected in our scenario relative to the $\gamma\gamma$ final state and where they stand vis-a-vis the experimental results. Such a study of relative strengths over the parameter space of our scenario would be indicative of how well the same is compatible with the experimental observations in the Higgs sector, in a global sense. The recent results from the ATLAS and the CMS collaborations on different decay modes of the lightest Higgs boson are presented in table 2. In fig. 10, we present the μ -values reported by the ATLAS and the CMS collaborations for different final states in the so-called signature (ratio) space, in reference to $\mu_{\gamma\gamma}$.

In each plot, the blue circle (green square) represents the experimentally reported central values for a given pair of observables from ATLAS and CMS collaborations, respectively. The solid grey lines show the range of μ values as observed by the CMS experiment while the dashed ones delineate the same as obtained by the ATLAS experiment. In order to generate fig. 10 we vary $\tan \beta$ within the range $10 < \tan \beta < 40$. We have also varied the

Channel	μ (CMS)	μ (ATLAS)
$h \rightarrow \gamma\gamma$	$1.14^{+0.26}_{-0.23}$ [4]	$1.17^{+0.27}_{-0.27}$ [3]
$h \xrightarrow{ZZ^*} 4l$	$0.93^{+0.39}_{-0.32}$ [123]	$1.44^{+0.40}_{-0.33}$ [3]
$h \xrightarrow{WW^*} 2l2\nu$	$0.72^{+0.20}_{-0.18}$ [124]	$1.0^{+0.30}_{-0.30}$ [125]
$h \rightarrow b\bar{b}$	$1.0^{+0.5}_{-0.5}$ [126]	$0.2^{+0.70}_{-0.60}$ [127]
$h \rightarrow \tau\bar{\tau}$	$0.78^{+0.27}_{-0.27}$ [128]	$1.4^{+0.5}_{-0.4}$ [129]

Table 2. Signal strengths (μ) in different decay final states of the SM-like Higgs boson as reported by the CMS and the ATLAS collaborations (with the corresponding references).

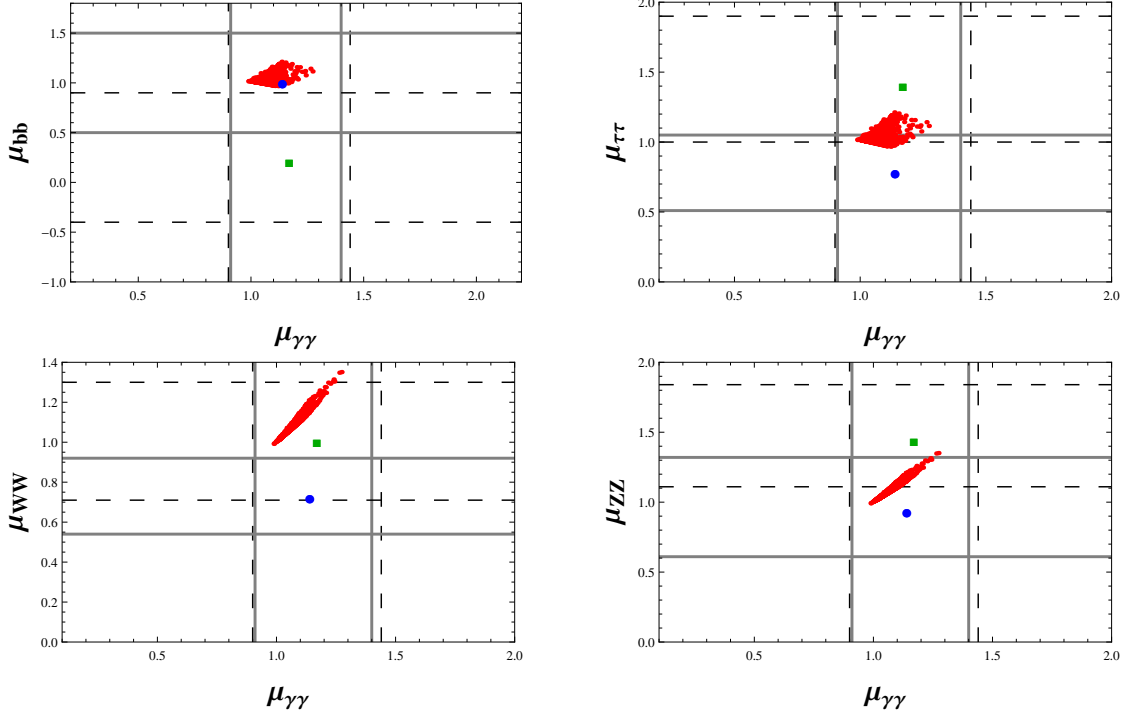


Figure 10. Bands representing mutual variation of relative signal strengths in various possible final states arising from the decay of the lightest Higgs boson as obtained by scanning the parameter space of the scenario under consideration. The ranges of different parameters used in the scan are as follows: $10 < \tan\beta < 40$, $350 \text{ GeV} < m_{\tilde{t}} < 1.5 \text{ TeV}$, $0.1 < f < 1$ and $0.1 < \lambda_T < 0.55$. The solid grey lines give $1\text{-}\sigma$ ranges from the MVA based analysis (main analysis) performed by the CMS collaboration (blue circles represent the respective central values) whereas the dashed grey lines represent the corresponding results from the ATLAS collaboration (green squares represent the respective central values).

mass of the top squark within the range $350 \text{ GeV} < m_{\tilde{t}} < 1.5 \text{ TeV}$ with $0.1 < f < 1$ and $0.1 < \lambda_T < 0.55$. All other parameters are kept fixed at the previously mentioned values in section 5.2. While scanning, care has been taken to reject spectra with tachyonic scalar states and to conform with the lower bound on the lightest chargino mass of 104 GeV as obtained from the LEP experiment. Also, the scan required m_h to be within the range of 124.0 – 126.2 GeV as reported by the LHC experiments. The spread in the upper two plots

in fig. 10 are due to the variation of f which affects μ_{bb} and $\mu_{\gamma\gamma}$ whereas μ_{WW} and μ_{ZZ} remain unaffected. The values of $\mu_{\gamma\gamma}$ is very much consistent with the recent ATLAS and CMS findings. Finally, in order to have an idea of the mass-spectra of the light neutralino and the chargino states, we provide a few benchmark points in table 3, for the large ‘ f ’ scenario.

Parameters	BP-1	BP-2	BP-3
M_1^D	1500 GeV	1000 GeV	1200 GeV
M_2^D	1500.1 GeV	1000.1 GeV	1200.1 GeV
μ_u	200 GeV	200 GeV	200 GeV
$m_{3/2}$	20 GeV	20 GeV	10 GeV
$\tan\beta$	25	35	40
$m_{\tilde{t}}$	500 GeV	400 GeV	400 GeV
f	0.8	0.8	0.8
λ_T	0.5	0.52	0.52
v_S	10^{-4} GeV	10^{-4} GeV	10^{-4} GeV
v_T	10^{-3} GeV	10^{-3} GeV	10^{-3} GeV
$B\mu_L$	$-(400)^2$ (GeV) ²	$-(400)^2$ (GeV) ²	$-(400)^2$ (GeV) ²
Observables	BP-1	BP-2	BP-3
m_h	124.98 GeV	125.45 GeV	125.73 GeV
$(m_\nu)_{\text{Tree}}$	0.04 eV	0.1 eV	0.08 eV
$m_{\tilde{\chi}_7^0}$	168 MeV	169 MeV	84 MeV
$m_{\tilde{\chi}_6^0}$	208.73 GeV	210.58 GeV	209.75 GeV
$m_{\tilde{\chi}_5^0}$	208.74 GeV	210.59 GeV	209.76 GeV
$m_{\tilde{\chi}_4^0}$	1504.17 GeV	1006.13 GeV	1205.29 GeV
$m_{\tilde{\chi}_3^0}$	1504.23 GeV	1006.19 GeV	1205.31 GeV
$m_{\tilde{\chi}_2^0}$	1.19×10^5 GeV	1.11×10^5 GeV	1.33×10^5 GeV
$m_{\tilde{\chi}_1^0}$	1.19×10^5 GeV	1.11×10^5 GeV	1.33×10^5 GeV
$m_{\tilde{\chi}_3^+}$	208.13 GeV	211.91 GeV	210.24 GeV
$m_{\tilde{\chi}_2^+}$	1500.11 GeV	1000.11 GeV	1200.1 GeV
$m_{\tilde{\chi}_1^+}$	1508.27 GeV	1012.15 GeV	1210.45 GeV
$\mu_{\gamma\gamma}$	1.07	1.11	1.11

Table 3. Benchmark sets of input parameters in the large Yukawa coupling (f) scenario and the resulting mass-values for some relevant excitations. The Higgs signal strength in the diphoton final state ($\mu_{\gamma\gamma}$) is also indicated.

6.2 The case of small Yukawa coupling, $f \sim \mathcal{O}(10^{-4})$

In the limit when the Yukawa coupling is small ($f \sim 10^{-4}$), the next-to-lightest neutralino state becomes the sterile neutrino with negligible active-sterile mixing. The lightest neutralino state is again the active neutrino. The tree level Majorana mass of the active neutrino is given by eq. (4.11) whereas the sterile neutrino mass and the mixing angle

between the active and the sterile neutrino are given by eqs. (4.13) and (4.14). We have mentioned in the previous section that an X-ray line at around 3.5 keV was observed in the X-ray spectra of the Andromeda galaxy and in the same from various other galaxy clusters including the Perseus cluster. The observed flux and the best fit energy peak are shown in [130, 131]. The origin of this line is disputed since atomic transitions in the thermal plasma may also be responsible for this energy line. Nevertheless, a possible explanation can be provided by taking into account a 7 keV dark matter, in this case a sterile neutrino [130, 131]. As discussed earlier, the observed flux and the peak of the energy can be translated to an active-sterile mixing in the range $2.2 \times 10^{-11} < \sin^2 2\theta_{14} < 2 \times 10^{-10}$. To satisfy such small active sterile mixing, the tree level neutrino mass turns out to be very small ($\mathcal{O}(10^{-5})$ eV). Therefore, in order to explain the neutrino mass and mixing, one needs to invoke radiative corrections. For a detailed discussion, we refer the reader to [88]. It is also important to study the signal strength of $h \rightarrow \gamma\gamma$ in the light of this 7 keV sterile neutrino with appropriate active-sterile mixing.

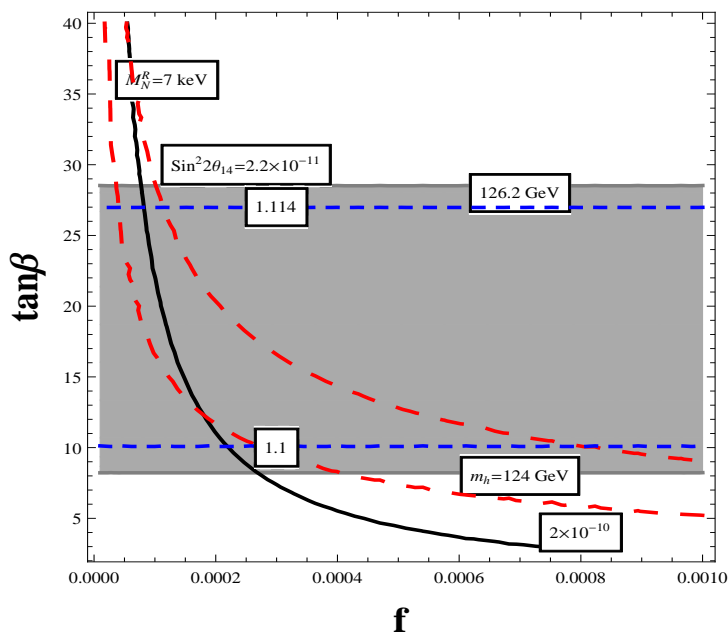


Figure 11. Contours of fixed values of m_h , $\mu_{\gamma\gamma}$, M_N^R and $\sin^2 2\theta_{14}$ in the $f - \tan\beta$ parameter space. The respective values of the contour lines are as shown in the figure. The shaded region in grey corresponds to the experimentally allowed band of the lightest Higgs boson mass. Other parameters are fixed at values mentioned in the text.

In fig. 11 we present the contours of m_h , $\mu_{\gamma\gamma}$, M_N^R and $\sin^2 2\theta_{14}$ in the $f - \tan\beta$ plane. The contour of the sterile neutrino mass of 7 keV is shown with the thick black line. The red dashed lines represent the contours of active-sterile mixing fixed at 2.2×10^{-11} and 2×10^{-10} . We have fixed M_1^D at 1 TeV, maintaining a degeneracy $\epsilon = (M_2^D - M_1^D) = 10^{-4}$ GeV. μ_u is fixed at 500 GeV. The other fixed parameters are $m_{3/2} = 10$ GeV, $m_{\tilde{t}} = 400$ GeV, $\lambda_T = 0.57$, $v_S = -0.01$ GeV, $v_T = 0.01$ GeV and $B\mu_L = -(400)^2 (\text{GeV})^2$. The not so

heavy top squark, as justified in section 6.1.2, enhances $\mu_{\gamma\gamma}$ considerably and we show the contours of $\mu_{\gamma\gamma}$ at 1.1 and 1.114 respectively with blue dashed lines. Finally, the grey shaded region is the parameter space consistent with the observed Higgs boson mass $124.0 \text{ GeV} < m_h < 126.2 \text{ GeV}$. Figure 11 clearly shows that for this choice of parameters $\mu_{\gamma\gamma} \gtrsim 1.1$ is completely consistent with a 7 keV sterile neutrino dark matter and the experimentally allowed range of Higgs boson mass. We have seen that charginos do not provide much enhancement to $\mu_{\gamma\gamma}$ due to its very suppressed couplings under the present set-up. Furthermore, avoiding possible appearance of tachyonic scalar states restricts the v_{ev} of the singlet from becoming large. Therefore, expecting an enhancement in $\mu_{\gamma\gamma}$ via suppression of the $hb\bar{b}$ coupling because of the singlet admixture seems unrealistic. Thus, the only enhancement in $\mu_{\gamma\gamma}$ can come from light top squarks. In addition, large radiative corrections from λ_S and λ_T reduces the necessity of having heavy top squarks. In the scatter plot of fig. 12 we show the possible range of variation of $\mu_{\gamma\gamma}$ with varying $m_{\tilde{t}}$. To

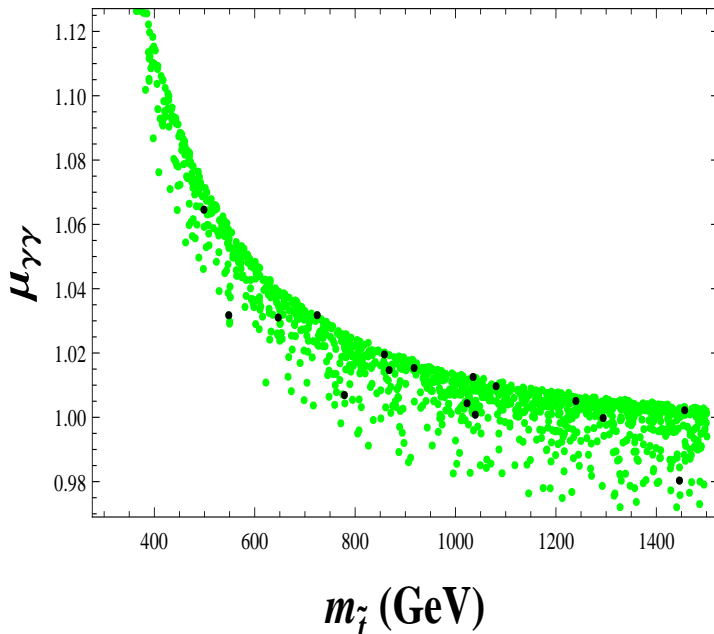


Figure 12. Scatter plot showing possible range of variation of $\mu_{\gamma\gamma}$ with varying $m_{\tilde{t}}$. The blue points are consistent with $7.01 \text{ keV} < M_N^R < 7.11 \text{ keV}$. All points satisfy $124.0 \text{ GeV} < m_h < 126.2 \text{ GeV}$.

generate this plot we have chosen relevant parameters over the following ranges: $1 \text{ GeV} < m_{3/2} < 20 \text{ GeV}$, $5 < \tan\beta < 40$, $300 \text{ GeV} < m_{\tilde{t}} < 1.5 \text{ TeV}$, $10^{-5} < f < 3 \times 10^{-4}$, $0.1 < \lambda_T < 1$ and $-0.01 \text{ GeV} < v_S < -1 \text{ GeV}$. Other parameters are retained at their previously mentioned values (used to obtain fig. 11), maintaining the degeneracy between the Dirac gaugino masses as already mentioned. Again, all these points are consistent with $124.0 \text{ GeV} < m_h < 126.2 \text{ GeV}$ and free from any tachyonic scalar states. The effects of the light top squarks results in some enhancement in $\mu_{\gamma\gamma}$. The blue points are consistent with a keV sterile neutrino with mass ranging between $7.01 \text{ keV} < M_N^R < 7.11 \text{ keV}$ and is known

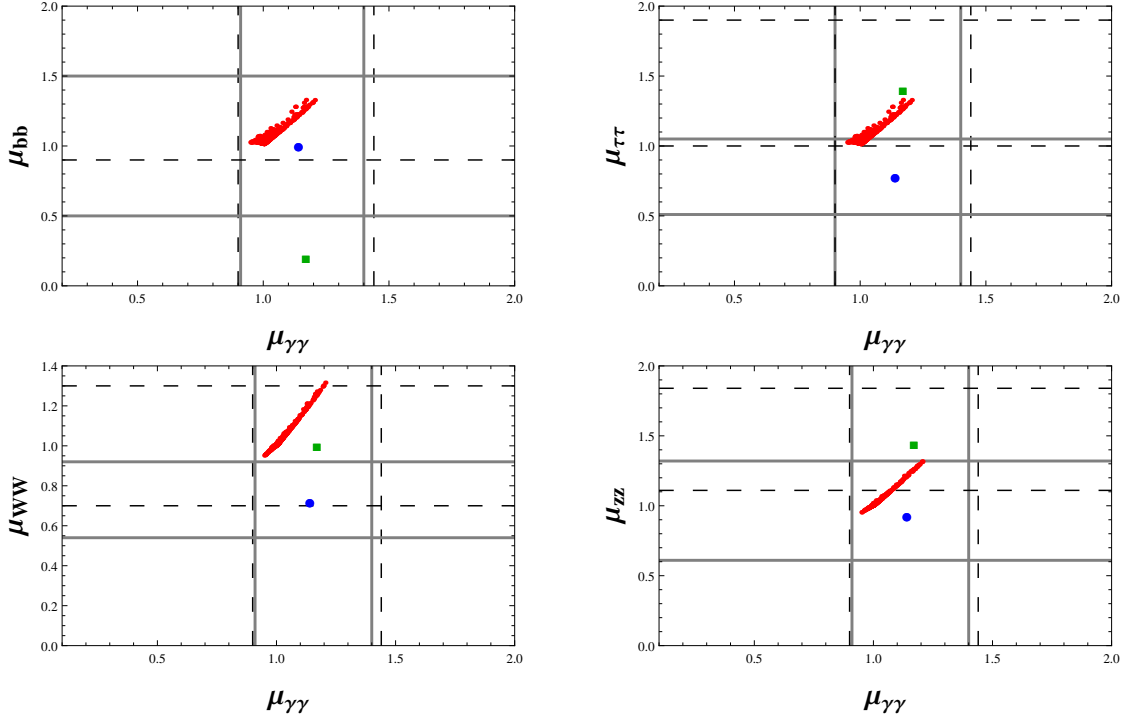


Figure 13. Same as in figure 10 except for a small input value of f .

to be a fit warm dark matter candidate having the right relic density. Finally, it is again very relevant to check the relative signal strengths for different decay modes of the lightest Higgs boson in such a scenario with small ‘ f ’; similar to what we have done in section 6.1.3 for the large ‘ f ’ scenario. Figure 13 shows scattered points consistent with the CMS or/and the ATLAS results at 1σ level. However, note that the scatter plot in the $\mu_{\gamma\gamma}-\mu_{WW}$ plane is consistent only with the results from the ATLAS experiments at the 1σ level whereas the scatter plot in the $\mu_{\gamma\gamma}-\mu_{bb}$ plane is consistent only with the results from the CMS experiments at the 1σ level. In the near future, a more precise measurement together with an improved analysis is likely to become more decisive on this issue. Finally, for the sake of completeness, in table 4 we provide three more benchmark sets comprising of the input parameters of the small Yukawa coupling scenario (with ($f \sim 10^{-4}$)), the corresponding mass-values of the relevant excitations and the Higgs signal strengths in the diphoton final state ($\mu_{\gamma\gamma}$).

7 Concluding remarks

In this paper we study the $h \rightarrow \gamma\gamma$ channel in the $U(1)_R$ lepton number model with a right handed neutrino. We show that the recent results from ATLAS and CMS on $\mu_{\gamma\gamma}$ is very much consistent with our outcomes for both the cases, i.e., $f \sim \mathcal{O}(1)$ and $f \sim \mathcal{O}(10^{-4})$. We also show for large neutrino Yukawa coupling, f the light bino-like neutralino state is not yet constrained from the invisible branching fraction of the Higgs boson.

Parameters	BP-4	BP-5	BP-6
M_1^D	1000 GeV	900 GeV	1200 GeV
μ_u	300 GeV	600 GeV	600 GeV
$m_{3/2}$	4 GeV	10 GeV	15 GeV
$\tan \beta$	35	25	15
$m_{\tilde{t}}$	500 GeV	500 GeV	500 GeV
f	9.9×10^{-5}	8.9×10^{-5}	1.21×10^{-4}
λ_T	0.55	0.55	0.55
v_S	-10^{-2} GeV	-10^{-2} GeV	-10^{-2} GeV
v_T	10^{-2} GeV	10^{-2} GeV	10^{-2} GeV
Observables	BP-4	BP-5	BP-6
m_h	125 GeV	124.257 GeV	124.448 GeV
m_N^R	7.03 keV	7.09 keV	7.03 keV
$m_{\tilde{\chi}_6^0}$	292.375 GeV	571.91 GeV	587.24 GeV
$m_{\tilde{\chi}_5^0}$	292.376 GeV	571.92 GeV	587.25 GeV
$m_{\tilde{\chi}_4^0}$	1004.06 GeV	904.16 GeV	1203.24 GeV
$m_{\tilde{\chi}_3^0}$	1004.07 GeV	904.19 GeV	1203.28 GeV
$m_{\tilde{\chi}_2^0}$	1022.03 GeV	939.91 GeV	1222.84 GeV
$m_{\tilde{\chi}_1^0}$	1022.72 GeV	939.83 GeV	1222.72 GeV
$m_{\tilde{\chi}_3^+}$	311.56 GeV	609.77 GeV	608.27 GeV
$m_{\tilde{\chi}_2^+}$	1000.01 GeV	900.01 GeV	1200.02 GeV
$m_{\tilde{\chi}_1^+}$	1011.93 GeV	910.62 GeV	1208.7 GeV
$\sin^2 2\theta_{14}$	1.56×10^{-10}	4.7×10^{-11}	2.8×10^{-11}
$\mu_{\gamma\gamma}$	1.07	1.06	1.06

Table 4. Same as in table 3 but for small Yukawa coupling with $f \sim \mathcal{O}(10^{-4})$. In all three cases we have chosen $\epsilon = 10^{-4}$ GeV. Neutrino mass at the tree level is very small ($\mathcal{O}(10^{-5})$ eV) and not shown in the table (See text for more details).

So far we have seen that the model under consideration have already demonstrated its ability to attract constraints from recent experiments in diverse areas ranging from the neutrino to astro-particle physics and finally from the LHC experiments pertaining to the Higgs sector and other BSM searches. It will be really interesting to see if the model can provide any novel signatures as far as the collider experiments are concerned.

A The Higgs-chargino-chargino coupling

In this appendix we work out the Higgs-chargino-chargino coupling in the scenario under discussion and present the analytical expression for the width of the lightest Higgs boson decaying into a pair of charginos. The relevant Lagrangian in the two-component notation

containing the Higgs-chargino-chargino interaction is given by

$$\begin{aligned}
\mathcal{L}_{h\tilde{\chi}^+\tilde{\chi}^-} &= g \left(v_a + \frac{S_{i2}}{\sqrt{2}} h_i \right) \tilde{w}^+ e_L^- + \sqrt{2} \lambda_T \tilde{T}_u^+ \left(v_u + \frac{S_{i1}}{\sqrt{2}} h_i \right) \tilde{R}_d^- \\
&+ g \left(v_u + \frac{S_{i1}}{\sqrt{2}} h_i \right) \tilde{H}_u^+ \tilde{w}^- - \lambda_S \left(v_S + \frac{S_{i3}}{\sqrt{2}} h_i \right) \tilde{H}_u^+ \tilde{R}_d^- \\
&+ \lambda_T \left(v_T + \frac{S_{i4}}{\sqrt{2}} h_i \right) \tilde{H}_u^+ \tilde{R}_d^- + g \left(v_T + \frac{S_{i4}}{\sqrt{2}} h_i \right) \tilde{T}_u^+ \tilde{w}^- \\
&- g \left(v_T + \frac{S_{i4}}{\sqrt{2}} h_i \right) \tilde{w}^+ \tilde{T}_d^- + h.c., \tag{A.1}
\end{aligned}$$

where the matrix S connects the mass and gauge eigenstates of the CP even scalar mass squared matrix, written in the basis $(h_R, \tilde{\nu}_R, S_R, T_R)$. To be more precise the physical CP-even scalar states are related to the gauge eigenstates in the following manner:

$$\begin{pmatrix} h_1 \\ h_2 \\ h_3 \\ h_4 \end{pmatrix} = \begin{pmatrix} S_{11} & S_{12} & S_{13} & S_{14} \\ S_{21} & S_{22} & S_{23} & S_{24} \\ S_{31} & S_{32} & S_{33} & S_{34} \\ S_{41} & S_{42} & S_{43} & S_{44} \end{pmatrix} \begin{pmatrix} h_R \\ \tilde{\nu}_R \\ S_R \\ T_R \end{pmatrix}. \tag{A.2}$$

In our notation the lightest physical state (h_4) of the CP even scalar mass matrix corresponds to the physical Higgs boson, h . Moreover, the charginos $\tilde{\chi}_i^\pm$ are four component Dirac fermions which arise due to the mixing between the charged gauginos and higgsinos as well as the charged lepton of first generation. In order to evaluate find out the Higgs-chargino-chargino coupling and to evaluate the Higgs boson partial decay width to a pair of charginos, it is pertinent to write down the interaction Lagrangian in the four-component notation. We now define the 4-component spinors as

$$\tilde{W} = \begin{pmatrix} \tilde{w}^+ \\ \tilde{w}^- \end{pmatrix}, \quad \tilde{H} = \begin{pmatrix} \tilde{H}_u^+ \\ \tilde{R}_d^- \end{pmatrix}, \quad \tilde{T} = \begin{pmatrix} \tilde{T}_u^+ \\ \tilde{T}_d^- \end{pmatrix}, \quad L_e^{(4)} = \begin{pmatrix} e_R^c \\ \tilde{e}_L^- \end{pmatrix}. \tag{A.3}$$

Using the transformation relations,

$$\begin{aligned}
\tilde{w}^+ e_L^- &= \bar{L}_e^{(4)} P_L \tilde{W} \\
\tilde{T}_u^+ \tilde{R}_d^- &= \bar{\tilde{H}} P_L \tilde{T} \\
\tilde{H}_u^+ \tilde{w}^- &= \bar{\tilde{W}} P_L \tilde{H} \\
\tilde{H}_u^+ \tilde{R}_d^- &= \bar{\tilde{H}} P_L \tilde{H}, \tag{A.4}
\end{aligned}$$

the Lagrangian in eq. (A.1) can be expressed in the four component notation as

$$\begin{aligned}
\mathcal{L}_{h\tilde{\chi}^+\tilde{\chi}^-}^{(4)} &= g \frac{S_{42}}{\sqrt{2}} h \bar{L}_e^{(4)} P_L \tilde{W} + \sqrt{2} \lambda_T \frac{S_{41}}{\sqrt{2}} h \bar{\tilde{H}} P_L \tilde{T} + g \frac{S_{41}}{\sqrt{2}} h \bar{\tilde{W}} P_L \tilde{H} - \lambda_S \frac{S_{43}}{\sqrt{2}} h \bar{\tilde{H}} P_L \tilde{H} \\
&+ \lambda_T \frac{S_{44}}{\sqrt{2}} h \bar{\tilde{H}} P_L \tilde{H} + g \frac{S_{44}}{\sqrt{2}} h \bar{\tilde{W}} P_L \tilde{T} - g \frac{S_{44}}{\sqrt{2}} \bar{\tilde{T}} P_L \tilde{W} + h.c. \tag{A.5}
\end{aligned}$$

The chargino masses can have any sign. By demanding that the four component Lagrangian contains only positive masses for the charginos, we define the chargino states in the following manner [132, 133]

$$\tilde{\chi}_i^+ = (\epsilon_i P_L + P_R) \begin{pmatrix} \chi_i^+ \\ \tilde{\chi}_i^- \end{pmatrix}, \quad i = 1, \dots, 4 \quad (\text{A.6})$$

where ϵ_i carries the sign of the chargino masses, which can be ± 1 . When $\epsilon = -1$, $P_R - P_L = \gamma_5$, which essentially implies a γ_5 rotation to the four component spinors to absorb the sign. Hence, the transformation relations involving only P_L changes, which modifies the Feynman rules. The two-component mass eigenstates (χ_i^\pm) of the charginos are related to the gauge eigenstates in a manner shown in eq. (4.17).

Using the following set of relations

$$\begin{aligned} P_L \tilde{W} &= P_L V_{i1}^* \epsilon_i \tilde{\chi}_i \\ P_L \tilde{T} &= P_L V_{i2}^* \epsilon_i \tilde{\chi}_i \\ P_L \tilde{H} &= P_L V_{i3}^* \epsilon_i \tilde{\chi}_i \\ P_R \tilde{W} &= P_R U_{i1} \tilde{\chi}_i \\ P_R \tilde{H} &= P_R U_{i3} \tilde{\chi}_i \\ P_R \tilde{T} &= P_R U_{i2} \tilde{\chi}_i \\ P_R L_e^{(4)} &= P_R U_{i4} \tilde{\chi}_i, \end{aligned} \quad (\text{A.7})$$

we rewrite eq. (A.5) in the mass eigenstate basis as

$$\mathcal{L}_{h\tilde{\chi}_i^+ \tilde{\chi}_j^-}^{(4)m} = gh \tilde{\chi}_i^- (\zeta_{ij}^* P_L + \zeta_{ji} P_R) \tilde{\chi}_j, \quad (\text{A.8})$$

where

$$\begin{aligned} \zeta_{ij} &= \left[\frac{S_{42}}{\sqrt{2}} U_{i4} V_{j1} + \sqrt{2} \frac{\lambda_T}{g} \frac{S_{41}}{\sqrt{2}} U_{i3} V_{j2} + \frac{S_{41}}{\sqrt{2}} U_{i1} V_{j3} - \frac{\lambda_S}{g} \frac{S_{43}}{\sqrt{2}} U_{i3} V_{j3} \right. \\ &\quad \left. + \frac{\lambda_T}{g} \frac{S_{44}}{\sqrt{2}} U_{i3} V_{j3} + \frac{S_{44}}{\sqrt{2}} U_{i1} V_{j2} - \frac{S_{44}}{\sqrt{2}} U_{i2} V_{j1} \right] \epsilon_i. \end{aligned} \quad (\text{A.9})$$

The coupling is obtained from Eq. (A.8) as

$$\frac{g}{2} [\zeta_{ij}^* (1 - \gamma_5) + \zeta_{ji} (1 + \gamma_5)]. \quad (\text{A.10})$$

It is now straightforward to compute the lightest Higgs boson decay width to a pair of charginos, which we find as

$$\begin{aligned} \Gamma_{h \rightarrow \tilde{\chi}_i^+ \tilde{\chi}_j^-} &= \frac{g^2}{16\pi m_h^3} \left[\{m_h^2 - (m_{\tilde{\chi}_i^+}^2 + m_{\tilde{\chi}_j^-}^2)\}^2 - 4m_{\tilde{\chi}_i^+}^2 m_{\tilde{\chi}_j^-}^2 \right]^{1/2} \\ &\quad \left[(\zeta_{ij}^2 + \zeta_{ji}^2) (m_h^2 - m_{\tilde{\chi}_i^+}^2 - m_{\tilde{\chi}_j^-}^2) - 4\zeta_{ij} \zeta_{ji} m_{\tilde{\chi}_i^+} m_{\tilde{\chi}_j^-} \right]. \end{aligned} \quad (\text{A.11})$$

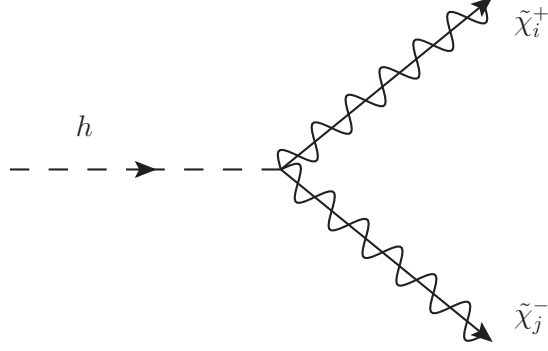


Figure 14. The Higgs-chargino-chargino vertex.

Finally, if we assume the singlet and the triplet vev 's to be very small, this would imply that the singlet and triplet mixing in the light CP-even Higgs boson states become negligible. Under such an assumption, the CP even states can be written as

$$\begin{aligned}\tilde{\nu}_R &\simeq v_a + \frac{1}{\sqrt{2}}(H \cos \alpha - h \sin \alpha) \\ h_R &\simeq v_u + \frac{1}{\sqrt{2}}(H \sin \alpha + h \cos \alpha),\end{aligned}\tag{A.12}$$

where we have chosen $S_{41} = \cos \alpha$, $S_{42} = -\sin \alpha$, and $S_{43} \sim S_{44} \sim 0$. With this simplification we can write

$$\begin{aligned}\zeta_{ij} &= \left[-\frac{\sin \alpha}{\sqrt{2}}U_{i4}V_{j1} + \frac{\cos \alpha}{\sqrt{2}}\left(\frac{\sqrt{2}\lambda_T}{g}U_{i3}V_{j2} + U_{i1}V_{j3}\right) \right] \epsilon_i \\ &= \xi_{ij} \sin \alpha - \eta_{ij} \cos \alpha,\end{aligned}\tag{A.13}$$

where

$$\begin{aligned}\xi_{ij} &= -\frac{U_{i4}V_{j1}}{\sqrt{2}}\epsilon_i \\ \eta_{ij} &= \frac{1}{\sqrt{2}}\left(\frac{\sqrt{2}\lambda_T}{g}U_{i3}V_{j2} + U_{i1}V_{j3}\right)\epsilon_i.\end{aligned}\tag{A.14}$$

B The Higgs-neutralino-neutralino coupling

In a similar manner the interaction of the Higgs boson with neutralinos can be constructed from the following (two-component) Lagrangian

$$\begin{aligned}
\mathcal{L}_{h\tilde{\chi}^0\tilde{\chi}^0} = & \frac{g'}{\sqrt{2}} \left(v_u + \frac{S_{i1}}{\sqrt{2}} h_i \right) \tilde{b} \tilde{H}_u^0 - \frac{g'}{\sqrt{2}} \left(v_a + \frac{S_{i2}}{\sqrt{2}} h_i \right) \tilde{b} \nu_e + \lambda_S \left(v_u + \frac{S_{i1}}{\sqrt{2}} h_i \right) \tilde{S} \tilde{R}_d^0 \\
& - \frac{g}{\sqrt{2}} \left(v_u + \frac{S_{i1}}{\sqrt{2}} h_i \right) \tilde{w} \tilde{H}_u^0 + \frac{g}{\sqrt{2}} \left(v_a + \frac{S_{i2}}{\sqrt{2}} h_i \right) \tilde{w} \nu_e + \lambda_T \left(v_u + \frac{S_{i1}}{\sqrt{2}} h_i \right) \tilde{T} \tilde{R}_d^0 \\
& + \left[\lambda_S \left(v_s + \frac{S_{i3}}{\sqrt{2}} h_i \right) + \lambda_T \left(v_T + \frac{S_{i4}}{\sqrt{2}} h_i \right) \right] \tilde{R}_d^0 \tilde{H}_u^0 - f \left(v_a + \frac{S_{i2}}{\sqrt{2}} h_i \right) \tilde{H}_u^0 N^c \\
& - f \left(v_u + \frac{S_{i1}}{\sqrt{2}} h_i \right) N^c \nu_e + h.c.
\end{aligned} \tag{B.1}$$

We stick to the notation for the lightest CP even physical scalar state being denoted by h_4 and identified with the lightest Higgs boson h . We again define the 4-component spinors as [134]

$$\begin{aligned}
\tilde{B} &= \begin{pmatrix} \tilde{b} \\ \tilde{\tau}^T \\ \tilde{b} \end{pmatrix}, \quad \tilde{S} = \begin{pmatrix} \tilde{S} \\ \tilde{\tau}^T \\ \tilde{S} \end{pmatrix}, \quad \tilde{R}_d = \begin{pmatrix} \tilde{R}_d^0 \\ \tilde{\tau}^0 \\ \tilde{R}_d \end{pmatrix}, \quad \tilde{H}_u = \begin{pmatrix} \tilde{H}_u^0 \\ \tilde{\tau}^0 \\ \tilde{H}_u \end{pmatrix}, \\
\tilde{T} &= \begin{pmatrix} \tilde{T} \\ \tilde{\tau}^T \\ \tilde{T} \end{pmatrix}, \quad \tilde{W} = \begin{pmatrix} \tilde{W} \\ \tilde{\tau}^T \\ \tilde{W} \end{pmatrix}, \quad \nu_e = \begin{pmatrix} \nu_e \\ \tilde{\nu}_e^T \end{pmatrix}, \quad N^c = \begin{pmatrix} N^c \\ \tilde{N}^{cT} \end{pmatrix}.
\end{aligned} \tag{B.2}$$

In terms of these spinors the 4-component Lagrangian takes the following form

$$\begin{aligned}
\mathcal{L}_{h\tilde{\chi}^0\tilde{\chi}^0}^{(4)} = & \frac{g'}{\sqrt{2}} \frac{S_{41}}{\sqrt{2}} h \tilde{B} P_L \tilde{H}_u - \frac{g'}{\sqrt{2}} \frac{S_{42}}{\sqrt{2}} h \tilde{B} P_L \nu_e + \lambda_S \frac{S_{41}}{\sqrt{2}} h \tilde{S} P_L \tilde{R}_d - \frac{g}{\sqrt{2}} \frac{S_{41}}{\sqrt{2}} h \tilde{W} P_L \tilde{H}_u \\
& + \frac{g}{\sqrt{2}} \frac{S_{42}}{\sqrt{2}} h \tilde{W} P_L \nu_e + \lambda_T \frac{S_{41}}{\sqrt{2}} h \tilde{T} P_L \tilde{R}_d + \lambda_S \frac{S_{43}}{\sqrt{2}} h \tilde{R}_d P_L \tilde{H}_u + \lambda_T \frac{S_{44}}{\sqrt{2}} h \tilde{R}_d P_L \tilde{H}_u \\
& - f \frac{S_{42}}{\sqrt{2}} h \tilde{H}_u P_L N^c - f \frac{S_{41}}{\sqrt{2}} h \tilde{N}^c P_L \nu_e + h.c.
\end{aligned} \tag{B.3}$$

Eq. (B.3) represents the interactions in the gauge eigenstate basis. Neutralinos are physical Majorana spinors, arising due to the mixing of the neutral gauginos, higgsinos as well as the active (first generation) and sterile neutrino states. The four component neutralino state is defined as

$$\tilde{\chi}_i^0 = (\epsilon_i P_L + P_R) \begin{pmatrix} \chi_i^0 \\ \tilde{\chi}_i^0 \end{pmatrix}, \quad i = 1, \dots, 8 \tag{B.4}$$

where χ_i^0 are two component neutralino mass eigenstates and they are related to the gauge eigenstates as

$$\chi_i^0 = N_{ij} \psi_j^0, \quad i, j = 1, \dots, 8 \tag{B.5}$$

where $\psi^0 = (\tilde{b}, \tilde{S}, \tilde{W}, \tilde{T}, \tilde{R}_d, \tilde{H}_u, N^c, \nu_e)^T$. As presented in Appendix A, in a similar fashion we use the following transformation relations to write down the interaction Lagrangian given in Eq. (B.3) in the mass eigenstate basis

$$\begin{aligned}
P_L \tilde{B} &= N_{i1}^* P_L \epsilon_i \tilde{\chi}_i^0, & P_R \tilde{B} &= N_{i1} P_R \tilde{\chi}_i^0 \\
P_L \tilde{S} &= N_{i2}^* P_L \epsilon_i \tilde{\chi}_i^0, & P_R \tilde{S} &= N_{i2} P_R \tilde{\chi}_i^0 \\
P_L \tilde{W} &= N_{i3}^* P_L \epsilon_i \tilde{\chi}_i^0, & P_R \tilde{W} &= N_{i3} P_R \tilde{\chi}_i^0 \\
P_L \tilde{T} &= N_{i4}^* P_L \epsilon_i \tilde{\chi}_i^0, & P_R \tilde{T} &= N_{i4} P_R \tilde{\chi}_i^0 \\
P_L \tilde{R}_d &= N_{i5}^* P_L \epsilon_i \tilde{\chi}_i^0, & P_R \tilde{R}_d &= N_{i5} P_R \tilde{\chi}_i^0 \\
P_L \tilde{H}_u &= N_{i6}^* P_L \epsilon_i \tilde{\chi}_i^0, & P_R \tilde{H}_u &= N_{i6} P_R \tilde{\chi}_i^0 \\
P_L N^c &= N_{i7}^* P_L \epsilon_i \tilde{\chi}_i^0, & P_R N^c &= N_{i7} P_R \tilde{\chi}_i^0 \\
P_L \nu_e &= N_{i8}^* P_L \epsilon_i \tilde{\chi}_i^0, & P_R \nu_e &= N_{i8} P_R \tilde{\chi}_i^0.
\end{aligned} \tag{B.6}$$

It is now straightforward to write down the Higgs-neutralino-neutralino interaction in the 4-component notation as

$$\mathcal{L}_{h\tilde{\chi}^0\tilde{\chi}^0}^{(4)m} = g\tilde{\chi}_i^0 h (\zeta_{ij}' P_L + \zeta_{ji}' P_R) \tilde{\chi}_j^0, \tag{B.7}$$

where

$$\begin{aligned}
\zeta_{ij}' &= S_{41} \left[\frac{g'}{g} \frac{N_{i1} N_{j6}}{2} + \frac{\lambda_S}{g} \frac{N_{i2} N_{j5}}{\sqrt{2}} - \frac{N_{i3} N_{j6}}{2} + \frac{\lambda_T}{g} \frac{N_{i4} N_{j5}}{\sqrt{2}} - \frac{f}{g} \frac{N_{i7} N_{j8}}{\sqrt{2}} \right] \epsilon_i \\
&+ S_{42} \left[\frac{N_{i3} N_{j8}}{2} - \frac{g'}{g} \frac{N_{i1} N_{j8}}{2} - \frac{f}{g} \frac{N_{i6} N_{j7}}{\sqrt{2}} \right] \epsilon_i + S_{43} \left[\frac{\lambda_S}{g} \frac{N_{i5} N_{j6}}{\sqrt{2}} \right] \epsilon_i \\
&+ S_{44} \left[\frac{\lambda_T}{g} \frac{N_{i5} N_{j6}}{\sqrt{2}} \right] \epsilon_i + (i \leftrightarrow j).
\end{aligned} \tag{B.8}$$

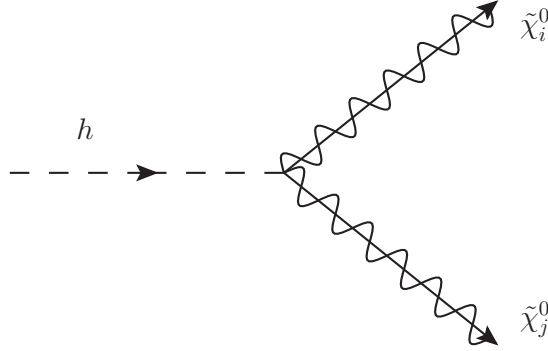


Figure 15. The Higgs-neutralino-neutralino vertex.

Finally, the partial decay width $\Gamma(h \rightarrow \tilde{\chi}_i^0 \tilde{\chi}_j^0)$ is given as

$$\begin{aligned}
\Gamma_{h \rightarrow \tilde{\chi}_i^0 \tilde{\chi}_j^0} &= \frac{g^2}{16\pi m_h^3 (1 + \delta_{ij})} \left[\{m_h^2 - (m_{\tilde{\chi}_i^0}^2 + m_{\tilde{\chi}_j^0}^2)\}^2 - 4m_{\tilde{\chi}_i^0}^2 m_{\tilde{\chi}_j^0}^2 \right]^{1/2} \times \\
&\left[(\zeta_{ij}'^2 + \zeta_{ji}'^2) (m_h^2 - m_{\tilde{\chi}_i^0}^2 - m_{\tilde{\chi}_j^0}^2) - 4\zeta_{ij}' \zeta_{ji}' m_{\tilde{\chi}_i^0} m_{\tilde{\chi}_j^0} \right].
\end{aligned} \tag{B.9}$$

Again in the limit where the singlet and triplet vev 's are very small, we can safely ignore the contributions from S_{43} and S_{44} . Furthermore, replacing S_{41} by $\cos \alpha$ and S_{42} by $-\sin \alpha$, we can write

$$\zeta'_{ij} = \eta'_{ij} \cos \alpha + \xi'_{ij} \sin \alpha, \quad (\text{B.10})$$

where,

$$\begin{aligned} \eta'_{ij} &= \left[\frac{g'}{g} \frac{N_{i1}N_{j6}}{2} + \frac{\lambda_S}{g} \frac{N_{i2}N_{j5}}{\sqrt{2}} - \frac{N_{i3}N_{j6}}{2} + \frac{\lambda_T}{g} \frac{N_{i4}N_{j5}}{\sqrt{2}} - \frac{f}{g} \frac{N_{i7}N_{j8}}{\sqrt{2}} \right] \epsilon_i + (i \leftrightarrow j), \\ \xi'_{ij} &= \left[\frac{g'}{g} \frac{N_{i1}N_{j8}}{2} + \frac{f}{g} \frac{N_{i6}N_{j7}}{\sqrt{2}} - \frac{N_{i3}N_{j8}}{2} \right] \epsilon_i + (i \leftrightarrow j). \end{aligned} \quad (\text{B.11})$$

Acknowledgments

SC would like to thank the Council of Scientific and Industrial Research, Government of India for the financial support received as a Senior Research Fellow. AD acknowledges the hospitality of the Department of Theoretical Physics, IACS during the course of this work. SR would like to thank the hospitality of the University of Helsinki and Helsinki Institute of Physics during the final stages of this work. It is also a pleasure to thank Dilip Kumar Ghosh, Katri Huitu and Oleg Lebedev for helpful discussions.

References

- [1] G. Aad *et al.* [ATLAS Collaboration], ‘‘Observation of a new particle in the search for the Standard Model Higgs boson with the ATLAS detector at the LHC,’’ *Phys. Lett. B* **716** (2012) 1 [arXiv:1207.7214 [hep-ex]].
- [2] S. Chatrchyan *et al.* [CMS Collaboration], ‘‘Observation of a new boson at a mass of 125 GeV with the CMS experiment at the LHC,’’ *Phys. Lett. B* **716** (2012) 30 [arXiv:1207.7235 [hep-ex]].
- [3] G. Aad *et al.* [ATLAS Collaboration], ‘‘Measurement of Higgs boson production in the diphoton decay channel in pp collisions at center-of-mass energies of 7 and 8 TeV with the ATLAS detector,’’ arXiv:1408.7084 [hep-ex].
- [4] V. Khachatryan *et al.* [CMS Collaboration], ‘‘Observation of the diphoton decay of the Higgs boson and measurement of its properties,’’ arXiv:1407.0558 [hep-ex].
- [5] A. Arbey, M. Battaglia, A. Djouadi and F. Mahmoudi, ‘‘An update on the constraints on the phenomenological MSSM from the new LHC Higgs results,’’ *Phys. Lett. B* **720** (2013) 153 [arXiv:1211.4004 [hep-ph]].
- [6] P. Bechtle, S. Heinemeyer, O. Stal, T. Stefaniak, G. Weiglein and L. Zeune, ‘‘MSSM Interpretations of the LHC Discovery: Light or Heavy Higgs?,’’ *Eur. Phys. J. C* **73** (2013) 2354 [arXiv:1211.1955 [hep-ph]].
- [7] K. Schmidt-Hoberg, F. Staub and M. W. Winkler, ‘‘Enhanced diphoton rates at Fermi and the LHC,’’ *JHEP* **1301** (2013) 124 [arXiv:1211.2835 [hep-ph]].
- [8] M. Drees, ‘‘A Supersymmetric Explanation of the Excess of Higgs–Like Events at the LHC and at LEP,’’ *Phys. Rev. D* **86** (2012) 115018 [arXiv:1210.6507 [hep-ph]].

- [9] A. Arbey, M. Battaglia, A. Djouadi and F. Mahmoudi, “The Higgs sector of the phenomenological MSSM in the light of the Higgs boson discovery,” *JHEP* **1209** (2012) 107 [arXiv:1207.1348 [hep-ph]].
- [10] K. Schmidt-Hoberg and F. Staub, “Enhanced $h \rightarrow \gamma\gamma$ rate in MSSM singlet extensions,” *JHEP* **1210** (2012) 195 [arXiv:1208.1683 [hep-ph]].
- [11] M. Carena, I. Low and C. E. M. Wagner, “Implications of a Modified Higgs to Diphoton Decay Width,” *JHEP* **1208** (2012) 060 [arXiv:1206.1082 [hep-ph]].
- [12] M. Carena, S. Gori, N. R. Shah and C. E. M. Wagner, “A 125 GeV SM-like Higgs in the MSSM and the $\gamma\gamma$ rate,” *JHEP* **1203** (2012) 014 [arXiv:1112.3336 [hep-ph]].
- [13] L. J. Hall, D. Pinner and J. T. Ruderman, “A Natural SUSY Higgs Near 126 GeV,” *JHEP* **1204** (2012) 131 [arXiv:1112.2703 [hep-ph]].
- [14] S. Heinemeyer, O. Stal and G. Weiglein, “Interpreting the LHC Higgs Search Results in the MSSM,” *Phys. Lett. B* **710** (2012) 201 [arXiv:1112.3026 [hep-ph]].
- [15] A. Arbey, M. Battaglia, A. Djouadi, F. Mahmoudi and J. Quevillon, “Implications of a 125 GeV Higgs for supersymmetric models,” *Phys. Lett. B* **708** (2012) 162 [arXiv:1112.3028 [hep-ph]].
- [16] P. Draper, P. Meade, M. Reece and D. Shih, “Implications of a 125 GeV Higgs for the MSSM and Low-Scale SUSY Breaking,” *Phys. Rev. D* **85** (2012) 095007 [arXiv:1112.3068 [hep-ph]].
- [17] N. Chen and H. -J. He, “LHC Signatures of Two-Higgs-Doublets with Fourth Family,” *JHEP* **1204** (2012) 062 [arXiv:1202.3072 [hep-ph]].
- [18] X. G. He, B. Ren and J. Tandean, “Hints of Standard Model Higgs Boson at the LHC and Light Dark Matter Searches,” *Phys. Rev. D* **85** (2012) 093019 [arXiv:1112.6364 [hep-ph]].
- [19] A. Djouadi, O. Lebedev, Y. Mambrini and J. Quevillon, “Implications of LHC searches for Higgs–portal dark matter,” *Phys. Lett. B* **709** (2012) 65 [arXiv:1112.3299 [hep-ph]].
- [20] K. Cheung and T. -C. Yuan, “Could the excess seen at 124–126 GeV be due to the Randall-Sundrum Radion?,” *Phys. Rev. Lett.* **108** (2012) 141602 [arXiv:1112.4146 [hep-ph]].
- [21] B. Batell, S. Gori and L. -T. Wang, “Exploring the Higgs Portal with 10/fb at the LHC,” *JHEP* **1206** (2012) 172 [arXiv:1112.5180 [hep-ph]].
- [22] N. D. Christensen, T. Han and S. Su, “MSSM Higgs Bosons at The LHC,” *Phys. Rev. D* **85** (2012) 115018 [arXiv:1203.3207 [hep-ph]].
- [23] A. Belyaev, S. Khalil, S. Moretti and M. C. Thomas, “Light sfermion interplay in the 125 GeV MSSM Higgs production and decay at the LHC,” *JHEP* **1405** (2014) 076 [arXiv:1312.1935 [hep-ph]].
- [24] M. Hameda, S. Khalil and S. Moretti, “Light chargino effects onto $h \rightarrow \gamma\gamma$ in the MSSM,” *Phys. Rev. D* **89** (2014) 1, 011701 [arXiv:1312.2504 [hep-ph]].
- [25] A. Chakraborty, B. Das, J. L. Diaz-Cruz, D. K. Ghosh, S. Moretti and P. Poullose, “The 125 GeV Higgs signal at the LHC in the CP Violating MSSM,” *Phys. Rev. D* **90** (2014) 055005 [arXiv:1301.2745 [hep-ph]].
- [26] S. F. King, M. Mühlleitner, R. Nevzorov and K. Walz, “Natural NMSSM Higgs Bosons,” *Nucl. Phys. B* **870** (2013) 323 [arXiv:1211.5074 [hep-ph]].
- [27] J. F. Gunion, Y. Jiang and S. Kraml, “Could two NMSSM Higgs bosons be present near 125 GeV?,” *Phys. Rev. D* **86** (2012) 071702 [arXiv:1207.1545 [hep-ph]].

- [28] G. Belanger, U. Ellwanger, J. F. Gunion, Y. Jiang, S. Kraml and J. H. Schwarz, “Higgs Bosons at 98 and 125 GeV at LEP and the LHC,” JHEP **1301** (2013) 069 [arXiv:1210.1976 [hep-ph]].
- [29] J. F. Gunion, Y. Jiang and S. Kraml, “The Constrained NMSSM and Higgs near 125 GeV,” Phys. Lett. B **710** (2012) 454 [arXiv:1201.0982 [hep-ph]].
- [30] U. Ellwanger and C. Hugonie, “Higgs bosons near 125 GeV in the NMSSM with constraints at the GUT scale,” Adv. High Energy Phys. **2012** (2012) 625389 [arXiv:1203.5048 [hep-ph]].
- [31] U. Ellwanger, “A Higgs boson near 125 GeV with enhanced di-photon signal in the NMSSM,” JHEP **1203** (2012) 044 [arXiv:1112.3548 [hep-ph]].
- [32] J. -J. Cao, Z. -X. Heng, J. M. Yang, Y. -M. Zhang and J. -Y. Zhu, “A SM-like Higgs near 125 GeV in low energy SUSY: a comparative study for MSSM and NMSSM,” JHEP **1203** (2012) 086 [arXiv:1202.5821 [hep-ph]].
- [33] Z. Kang, J. Li and T. Li, “On Naturalness of the MSSM and NMSSM,” JHEP **1211** (2012) 024 [arXiv:1201.5305 [hep-ph]].
- [34] K. Huitu and H. Waltari, “Higgs sector in NMSSM with right-handed neutrinos and spontaneous R-parity violation,” arXiv:1405.5330 [hep-ph].
- [35] S. Chatrchyan *et al.* [CMS Collaboration], “Search for microscopic black holes in pp collisions at $\sqrt{s} = 7$ TeV,” JHEP **1204** (2012) 061 [arXiv:1202.6396 [hep-ex]].
- [36] H. Baer, V. Barger and A. Mustafayev, “Implications of a 125 GeV Higgs scalar for LHC SUSY and neutralino dark matter searches,” Phys. Rev. D **85** (2012) 075010 [arXiv:1112.3017 [hep-ph]].
- [37] L. Aparicio, D. G. Cerdeno and L. E. Ibanez, “A 119-125 GeV Higgs from a string derived slice of the CMSSM,” JHEP **1204** (2012) 126 [arXiv:1202.0822 [hep-ph]].
- [38] J. Ellis and K. A. Olive, “Revisiting the Higgs Mass and Dark Matter in the CMSSM,” Eur. Phys. J. C **72** (2012) 2005 [arXiv:1202.3262 [hep-ph]].
- [39] H. Baer, V. Barger and A. Mustafayev, “Neutralino dark matter in mSUGRA/CMSSM with a 125 GeV light Higgs scalar,” JHEP **1205** (2012) 091 [arXiv:1202.4038 [hep-ph]].
- [40] J. Cao, Z. Heng, D. Li and J. M. Yang, “Current experimental constraints on the lightest Higgs boson mass in the constrained MSSM,” Phys. Lett. B **710** (2012) 665 [arXiv:1112.4391 [hep-ph]].
- [41] A. Elsayed, S. Khalil and S. Moretti, “Higgs Mass Corrections in the SUSY B-L Model with Inverse Seesaw,” Phys. Lett. B **715** (2012) 208 [arXiv:1106.2130 [hep-ph]].
- [42] L. Basso and F. Staub, “Enhancing $h \rightarrow \gamma\gamma$ with staus in SUSY models with extended gauge sector,” Phys. Rev. D **87** (2013) 015011 [arXiv:1210.7946 [hep-ph]].
- [43] S. Khalil and S. Moretti, “Heavy neutrinos, Z’ and Higgs bosons at the LHC: new particles from an old symmetry,” J. Mod. Phys. **4** (2013) 7 [arXiv:1207.1590 [hep-ph]].
- [44] S. Khalil and S. Moretti, “A simple symmetry as a guide toward new physics beyond the Standard Model,” Front. Phys. **1** (2013) 10 [arXiv:1301.0144 [physics.pop-ph]].
- [45] M. Frank, D. K. Ghosh, K. Huitu, S. K. Rai, I. Saha and H. Waltari, “Left-right supersymmetry after the Higgs discovery,” arXiv:1408.2423 [hep-ph].
- [46] M. Frank and S. Mondal, “Light Neutralino Dark Matter in $U(1)'$ models,” Phys. Rev. D **90** (2014) 075013 [arXiv:1408.2223 [hep-ph]].

- [47] T. Basak and S. Mohanty, “130 GeV gamma ray line and enhanced Higgs di-photon rate from Triplet-Singlet extended MSSM,” *JHEP* **1308** (2013) 020 [arXiv:1304.6856 [hep-ph]].
- [48] P. Fayet, “Supersymmetry and Weak, Electromagnetic and Strong Interactions,” *Phys. Lett. B* **64** (1976) 159.
- [49] J. Polchinski and L. Susskind, “Breaking Of Supersymmetry At Intermediate-Energy,” *Phys. Rev. D* **26**, 3661 (1982).
- [50] L. J. Hall, “Alternative Low-energy Supersymmetry,” *Mod. Phys. Lett. A* **5** (1990) 467.
- [51] L. J. Hall and L. Randall, “U(1)-R symmetric supersymmetry,” *Nucl. Phys. B* **352** (1991) 289.
- [52] I. Jack and D. R. T. Jones, “Nonstandard soft supersymmetry breaking,” *Phys. Lett. B* **457** (1999) 101 [hep-ph/9903365].
- [53] A. E. Nelson, N. Rius, V. Sanz and M. Unsal, “The Minimal supersymmetric model without a mu term,” *JHEP* **0208** (2002) 039 [hep-ph/0206102].
- [54] P. J. Fox, A. E. Nelson and N. Weiner, “Dirac gaugino masses and supersoft supersymmetry breaking,” *JHEP* **0208** (2002) 035 [hep-ph/0206096].
- [55] Z. Chacko, P. J. Fox and H. Murayama, “Localized supersoft supersymmetry breaking,” *Nucl. Phys. B* **706** (2005) 53 [hep-ph/0406142].
- [56] I. Antoniadis, K. Benakli, A. Delgado, M. Quiros and M. Tuckmantel, “Splitting extended supersymmetry,” *Phys. Lett. B* **634**, 302 (2006) [arXiv:hep-ph/0507192]; “Split extended supersymmetry from intersecting branes,” *Nucl. Phys. B* **744**, 156 (2006) [arXiv:hep-th/0601003].
- [57] I. Antoniadis, K. Benakli, A. Delgado and M. Quiros, “A new gauge mediation theory,” *Adv. Stud. Theor. Phys.* **2**, 645 (2008) [arXiv:hep-ph/0610265].
- [58] G. D. Kribs, E. Poppitz and N. Weiner, “Flavor in supersymmetry with an extended R-symmetry,” *Phys. Rev. D* **78** (2008) 055010 [arXiv:0712.2039 [hep-ph]].
- [59] S. Y. Choi, M. Drees, A. Freitas and P. M. Zerwas, “Testing the Majorana Nature of Gluinos and Neutralinos,” *Phys. Rev. D* **78** (2008) 095007 [arXiv:0808.2410 [hep-ph]].
- [60] S. D. L. Amigo, A. E. Blechman, P. J. Fox and E. Poppitz, “R-symmetric gauge mediation,” *JHEP* **0901**, 018 (2009) [arXiv:0809.1112 [hep-ph]]; A. E. Blechman, “R-symmetric Gauge Mediation and the MRSSM,” *Mod. Phys. Lett. A* **24** (2009) 633 [arXiv:0903.2822 [hep-ph]].
- [61] K. Benakli and M. D. Goodsell, “Dirac Gauginos in General Gauge Mediation,” *Nucl. Phys. B* **816** (2009) 185 [arXiv:0811.4409 [hep-ph]].
- [62] G. Belanger, K. Benakli, M. Goodsell, C. Moura and A. Pukhov, “Dark Matter with Dirac and Majorana Gaugino Masses,” *JCAP* **0908** (2009) 027 [arXiv:0905.1043 [hep-ph]].
- [63] K. Benakli and M. D. Goodsell, “Dirac Gauginos and Kinetic Mixing,” *Nucl. Phys. B* **830** (2010) 315 [arXiv:0909.0017 [hep-ph]].
- [64] A. Kumar, D. Tucker-Smith and N. Weiner, “Neutrino Mass, Sneutrino Dark Matter and Signals of Lepton Flavor Violation in the MRSSM,” *JHEP* **1009** (2010) 111 [arXiv:0910.2475 [hep-ph]].
- [65] B. A. Dobrescu and P. J. Fox, “Uplifted supersymmetric Higgs region,” *Eur. Phys. J. C* **70** (2010) 263 [arXiv:1001.3147 [hep-ph]].

- [66] K. Benakli and M. D. Goodsell, “Dirac Gauginos, Gauge Mediation and Unification,” Nucl. Phys. B **840** (2010) 1 [arXiv:1003.4957 [hep-ph]].
- [67] S. Y. Choi, D. Choudhury, A. Freitas, J. Kalinowski, J. M. Kim and P. M. Zerwas, “Dirac Neutralinos and Electroweak Scalar Bosons of $N=1/N=2$ Hybrid Supersymmetry at Colliders,” JHEP **1008** (2010) 025 [arXiv:1005.0818 [hep-ph]].
- [68] L. M. Carpenter, “Dirac Gauginos, Negative Supertraces and Gauge Mediation,” JHEP **1209** (2012) 102 [arXiv:1007.0017 [hep-th]].
- [69] G. D. Kribs, T. Okui and T. S. Roy, “Viable Gravity-Mediated Supersymmetry Breaking,” Phys. Rev. D **82** (2010) 115010 [arXiv:1008.1798 [hep-ph]].
- [70] S. Abel and M. Goodsell, “Easy Dirac Gauginos,” JHEP **1106** (2011) 064 [arXiv:1102.0014 [hep-th]].
- [71] K. Benakli, M. D. Goodsell and A. -K. Maier, “Generating μ and $B\mu$ in models with Dirac Gauginos,” Nucl. Phys. B **851** (2011) 445 [arXiv:1104.2695 [hep-ph]].
- [72] J. Kalinowski, “Phenomenology of R-symmetric supersymmetry,” Acta Phys. Polon. B **42** (2011) 2425.
- [73] K. Benakli, “Dirac Gauginos: A User Manual,” Fortsch. Phys. **59** (2011) 1079 [arXiv:1106.1649 [hep-ph]].
- [74] C. Frugiuele and T. Gregoire, “Making the Sneutrino a Higgs with a $U(1)_R$ Lepton Number,” Phys. Rev. D **85** (2012) 015016 [arXiv:1107.4634 [hep-ph]].
- [75] C. Brust, A. Katz, S. Lawrence and R. Sundrum, “SUSY, the Third Generation and the LHC,” JHEP **1203** (2012) 103 [arXiv:1110.6670 [hep-ph]].
- [76] K. Rehermann and C. M. Wells, “Weak Scale Leptogenesis, R-symmetry, and a Displaced Higgs,” arXiv:1111.0008 [hep-ph].
- [77] R. Davies and M. McCullough, “Small neutrino masses due to R-symmetry breaking for a small cosmological constant,” Phys. Rev. D **86** (2012) 025014 [arXiv:1111.2361 [hep-ph]].
- [78] H. Itoyama and N. Maru, “D-term Dynamical Supersymmetry Breaking Generating Split $N=2$ Gaugino Masses of Mixed Majorana-Dirac Type,” Int. J. Mod. Phys. A **27** (2012) 1250159 [arXiv:1109.2276 [hep-ph]].
H. Itoyama and N. Maru, “D-term Triggered Dynamical Supersymmetry Breaking,” Phys. Rev. D **88** (2013) 025012 [arXiv:1301.7548 [hep-ph], arXiv:1301.7548 [hep-ph]].
H. Itoyama and N. Maru, “126 GeV Higgs Boson Associated with D-term Triggered Dynamical Supersymmetry Breaking,” arXiv:1312.4157 [hep-ph].
- [79] E. Bertuzzo and C. Frugiuele, “Fitting Neutrino Physics with a $U(1)_R$ Lepton Number,” JHEP **1205** (2012) 100 [arXiv:1203.5340 [hep-ph]].
- [80] R. Davies, “Dirac gauginos and unification in F-theory,” JHEP **1210** (2012) 010 [arXiv:1205.1942 [hep-th]].
- [81] R. Argurio, M. Bertolini, L. Di Pietro, F. Porri and D. Redigolo, “Holographic Correlators for General Gauge Mediation,” JHEP **1208** (2012) 086 [arXiv:1205.4709 [hep-th]].
- [82] R. Fok, G. D. Kribs, A. Martin and Y. Tsai, “Electroweak Baryogenesis in R-symmetric Supersymmetry,” Phys. Rev. D **87** (2013) 5, 055018 [arXiv:1208.2784 [hep-ph]].
- [83] R. Argurio, M. Bertolini, L. Di Pietro, F. Porri and D. Redigolo, “Exploring Holographic General Gauge Mediation,” JHEP **1210** (2012) 179 [arXiv:1208.3615 [hep-th]].

- [84] C. Frugiuele, T. Gregoire, P. Kumar and E. Ponton, “‘L=R’ - $U(1)_R$ as the Origin of Leptonic ‘RPV,’” JHEP **1303** (2013) 156 [arXiv:1210.0541 [hep-ph]].
- [85] C. Frugiuele, T. Gregoire, P. Kumar and E. Ponton, “‘L=R’ - $U(1)_R$ Lepton Number at the LHC,” JHEP **1305** (2013) 012 [arXiv:1210.5257 [hep-ph]].
- [86] K. Benakli, M. D. Goodsell and F. Staub, “Dirac Gauginos and the 125 GeV Higgs,” JHEP **1306** (2013) 073 [arXiv:1211.0552 [hep-ph]].
- [87] F. Riva, C. Biggio and A. Pomarol, “Is the 125 GeV Higgs the superpartner of a neutrino?,” JHEP **1302** (2013) 081 [arXiv:1211.4526 [hep-ph]].
- [88] S. Chakraborty and S. Roy, “Higgs boson mass, neutrino masses and mixing and keV dark matter in an $U(1)_R$ - lepton number model,” JHEP **1401** (2014) 101 [arXiv:1309.6538 [hep-ph]].
- [89] C. Csaki, J. Goodman, R. Pavesi and Y. Shirman, “The $m_D - b_M$ Problem of Dirac Gauginos and its Solutions,” arXiv:1310.4504 [hep-ph].
- [90] E. Dudas, M. Goodsell, L. Heurtier and P. Tziveloglou, “Flavour models with Dirac and fake gluinos,” Nucl. Phys. B **884** (2014) 632 [arXiv:1312.2011 [hep-ph]].
- [91] H. Beauchesne and T. Gregoire, “Electroweak precision measurements in supersymmetric models with a $U(1)_R$ lepton number,” JHEP **1405** (2014) 051 [arXiv:1402.5403 [hep-ph]].
- [92] E. Bertuzzo, C. Frugiuele, T. Gregoire and E. Ponton, “Dirac gauginos, R symmetry and the 125 GeV Higgs,” arXiv:1402.5432 [hep-ph].
- [93] K. Benakli, M. Goodsell, F. Staub and W. Porod, “The Constrained Minimal Dirac Gaugino Supersymmetric Standard Model,” Phys. Rev. D **90**, 045017 (2014) [arXiv:1403.5122 [hep-ph]].
- [94] S. Chakraborty, D. K. Ghosh and S. Roy, “7 keV Sterile neutrino dark matter in $U(1)_R$ - lepton number model,” JHEP **1410** (2014) 146 [arXiv:1405.6967 [hep-ph]].
- [95] M. D. Goodsell and P. Tziveloglou, “Dirac Gauginos in Low Scale Supersymmetry Breaking,” arXiv:1407.5076 [hep-ph].
- [96] S. Ipek, D. McKeen and A. E. Nelson, “CP Violation in Pseudo-Dirac Fermion Oscillations,” arXiv:1407.8193 [hep-ph].
- [97] D. Busbridge, “Constrained Dirac gluino mediation,” arXiv:1408.4605 [hep-ph].
- [98] P. DieÅšner, J. Kalinowski, W. Kotlarski and D. StÅckinger, “Higgs boson mass and electroweak observables in the MRSSM,” arXiv:1410.4791 [hep-ph].
- [99] A. Merle, “keV Neutrino Model Building,” Int. J. Mod. Phys. D **22** (2013) 1330020 [arXiv:1302.2625 [hep-ph]].
- [100] H. K. Dreiner, S. Heinemeyer, O. Kittel, U. Langenfeld, A. M. Weber and G. Weiglein, “Mass Bounds on a Very Light Neutralino,” Eur. Phys. J. C **62** (2009) 547 [arXiv:0901.3485 [hep-ph]].
- [101] J. F. Gunion, D. Hooper and B. McElrath, “Light neutralino dark matter in the NMSSM,” Phys. Rev. D **73** (2006) 015011 [hep-ph/0509024].
- [102] H. K. Dreiner, J.S. Kim and O. Lebedev, “First LHC constraints on neutralinos,” Phys. Lett. B **715** (2012) 199 [arXiv:1206.3096] [inSPIRE].

- [103] L. Calibbi, J. M. Lindert, T. Ota and Y. Takanishi, “Cornering light Neutralino Dark Matter at the LHC,” *JHEP* **1310** (2013) 132 [arXiv:1307.4119].
- [104] H. K. Dreiner, M. Hanussek, J. S. Kim and S. Sarkar, “Gravitino cosmology with a very light neutralino,” *Phys. Rev. D* **85** (2012) 065027 [arXiv:1111.5715 [hep-ph]].
- [105] H. K. Dreiner, S. Grab, D. Koschade, M. Kramer, B. O’Leary and U. Langenfeld, “Rare meson decays into very light neutralinos,” *Phys. Rev. D* **80**, 035018 (2009) [arXiv:0905.2051 [hep-ph]].
- [106] D. Choudhury, H. K. Dreiner, P. Richardson and S. Sarkar, “A Supersymmetric solution to the KARMEN time anomaly,” *Phys. Rev. D* **61** (2000) 095009 [hep-ph/9911365].
- [107] R. Adhikari and B. Mukhopadhyaya, “Can we identify a light neutralino in B Factories?,” *Phys. Lett. B* **353** (1995) 228 [hep-ph/9411208].
- [108] R. Adhikari and B. Mukhopadhyaya, “Light neutralinos in B decays,” *Phys. Rev. D* **52** (1995) 3125 [hep-ph/9411347].
- [109] R. Adhikari and B. Mukhopadhyaya, “Some signals for a light neutralino,” hep-ph/9508256.
- [110] PARTICLE DATA GROUP collaboration, J. Beringer et al., *Review of particle physics*, *Phys. Rev. D* **86** (2012) 010001 [inSPIRE].
- [111] M. Kawasaki and T. Moroi, “Gravitino production in the inflationary universe and the effects on big bang nucleosynthesis,” *Prog. Theor. Phys.* **93** (1995) 879 [hep-ph/9403364][inSPIRE].
- [112] A. Boyarsky, O. Ruchayskiy and D. Iakubovskiy, “A Lower bound on the mass of Dark Matter particles,” *JCAP* **0903** (2009) 005 [arXiv:0808.3902 [hep-ph]].
- [113] A. Boyarsky, O. Ruchayskiy and M. Shaposhnikov, *Ann. Rev. Nucl. Part. Sci.* **59** (2009) 191 [arXiv:0901.0011 [hep-ph]].
- [114] A. Djouadi, “The Anatomy of electro-weak symmetry breaking. I: The Higgs boson in the standard model,” *Phys. Rept.* **457** (2008) 1 [hep-ph/0503172].
- [115] A. Djouadi, “The Anatomy of electro-weak symmetry breaking. II. The Higgs bosons in the minimal supersymmetric model,” *Phys. Rept.* **459** (2008) 1 [hep-ph/0503173].
- [116] M. Spira, “QCD effects in Higgs physics,” *Fortsch. Phys.* **46** (1998) 203 [hep-ph/9705337].
- [117] M. Spira, A. Djouadi, D. Graudenz and P. M. Zerwas, “Higgs boson production at the LHC,” *Nucl. Phys. B* **453** (1995) 17 [hep-ph/9504378].
- [118] W. -Y. Keung and W. J. Marciano, “Higgs Scalar Decays: $H \rightarrow W^+ X$,” *Phys. Rev. D* **30** (1984) 248.
- [119] T. G. Rizzo, “Decays of Heavy Higgs Bosons,” *Phys. Rev. D* **22** (1980) 722.
- [120] V. Khachatryan *et al.* [CMS Collaboration], “Constraints on the Higgs boson width from off-shell production and decay to Z-boson pairs,” *Phys. Lett. B* **736** (2014) 64 [arXiv:1405.3455 [hep-ex]].
- [121] K. Cheung, J. S. Lee and P. Y. Tseng, “Higgcision Updates 2014,” arXiv:1407.8236 [hep-ph].
- [122] W. Porod, M. Hirsch, J. Romao and J. W. F. Valle, *Phys. Rev. D* **63** (2001) 115004 doi:10.1103/PhysRevD.63.115004 [hep-ph/0011248].
- [123] S. Chatrchyan *et al.* [CMS Collaboration], “Measurement of the properties of a Higgs boson in the four-lepton final state,” *Phys. Rev. D* **89**, 092007 (2014) [arXiv:1312.5353 [hep-ex]].

- [124] S. Chatrchyan *et al.* [CMS Collaboration], “Measurement of Higgs boson production and properties in the WW decay channel with leptonic final states,” JHEP **1401**, 096 (2014) [arXiv:1312.1129 [hep-ex]].
- [125] [ATLAS Collaboration], “Combined coupling measurements of the Higgs-like boson with the ATLAS detector using up to 25 fb⁻¹ of proton-proton collision data,” ATLAS-CONF-2013-034.
- [126] S. Chatrchyan *et al.* [CMS Collaboration], “Search for the standard model Higgs boson produced in association with a W or a Z boson and decaying to bottom quarks,” Phys. Rev. D **89**, 012003 (2014) [arXiv:1310.3687 [hep-ex]].
- [127] The ATLAS collaboration, “Search for the bb decay of the Standard Model Higgs boson in associated W/ZH production with the ATLAS detector,” ATLAS-CONF-2013-079.
- [128] S. Chatrchyan *et al.* [CMS Collaboration], “Evidence for the 125 GeV Higgs boson decaying to a pair of τ leptons,” JHEP **1405**, 104 (2014) [arXiv:1401.5041 [hep-ex]].
- [129] The ATLAS collaboration, “Evidence for Higgs Boson Decays to the $\tau^+\tau^-$ Final State with the ATLAS Detector,” ATLAS-CONF-2013-108.
- [130] E. Bulbul, M. Markevitch, A. Foster, R. K. Smith, M. Loewenstein and S. W. Randall, arXiv:1402.2301 [astro-ph.CO].
- [131] A. Boyarsky, O. Ruchayskiy, D. Iakubovskiy and J. Franse, arXiv:1402.4119 [astro-ph.CO].
- [132] J. F. Gunion and H. E. Haber, “Higgs Bosons in Supersymmetric Models. 1.,” Nucl. Phys. B **272** (1986) 1 [Erratum-ibid. B **402** (1993) 567].
- [133] J. F. Gunion and H. E. Haber, “Higgs Bosons in Supersymmetric Models. 2. Implications for Phenomenology,” Nucl. Phys. B **278** (1986) 449.
- [134] M. Drees, R. Godbole and P. Roy, “Theory and phenomenology of sparticles: An account of four-dimensional N=1 supersymmetry in high energy physics,” Hackensack, USA: World Scientific (2004) 555 p